Journal of Advanced Research 64 (2024) 195–211

Contents lists available at ScienceDirect

Journal of Advanced Research

journal homepage: www.elsevier.com/locate/jare

Original Manuscript

Tetramethylpyrazine nitrone exerts neuroprotection via activation of PGC-1α/Nrf2 pathway in Parkinson's disease models

Baojian Guo [a,b,1], Chengyou Zheng [a,c,1], Jie Cao [a], Fangcheng Luo [a], Haitao Li [d], Shengquan Hu [e], Simon Mingyuan Lee [f], Xifei Yang [g], Gaoxiao Zhang [a], Zaijun Zhang [a,*], Yewei Sun [a,*], Yuqiang Wang [a]

[a] State Key Laboratory of Bioactive Molecules and Druggability Assessment, Guangzhou Key Laboratory of Innovative Chemical Drug Research in Cardio-cerebrovascular Diseases, and Institute of New Drug Research, Jinan University College of Pharmacy, Guangzhou 510632, China
[b] Integrated Chinese and Western Medicine Postdoctoral Research Station, Jinan University, Guangzhou 510632, China
[c] School of Chemical Biology and Biotechnology, Shenzhen Graduate School of Peking University, Shenzhen 518055, China
[d] Department of Bioengineering, Zhuhai Campus of Zunyi Medical University, Zhuhai 519041, China
[e] Shenzhen Institute of Translational Medicine/Shenzhen Institute of Gerontology, The First Affiliated Hospital of Shenzhen University, Shenzhen, Guangdong Province, China
[f] Institute of Chinese Medical Sciences and State Key Laboratory of Quality Research in Chinese Medicine, University of Macau, Avenida da Universidade, Taipa, Macao
[g] Key Laboratory of Modern Toxicology of Shenzhen, Center for Disease Control and Prevention, No. 8, Longyuan Road, Nanshan District, Shenzhen 518055, China

HIGHLIGHTS

- TBN exerts neuroprotection in different PD models.
- TBN alleviates oxidative damage and mitochondrial dysfunction.
- The therapeutic effect of TBN is associated with activation of PGC-1α/Nrf2 pathway.
- TBN is safe in Phase I study and could be a disease-modifying treatment for PD.

GRAPHICAL ABSTRACT

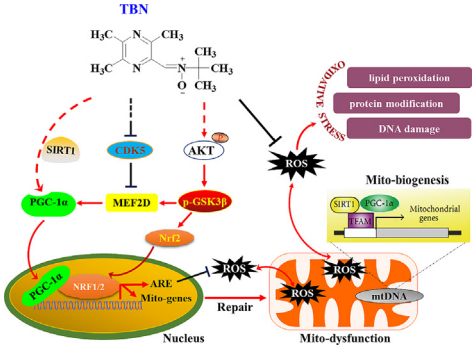

ARTICLE INFO

Article history:
Received 7 August 2022
Revised 17 November 2023
Accepted 17 November 2023
Available online 19 November 2023

Keywords:
Parkinson's disease
Tetramethylpyrazine nitrone
Peroxisome proliferator-activated receptor γ co-activator 1α
Nuclear factor erythroid-2-related factor 2

ABSTRACT

Introduction: Parkinson's disease (PD) is common neurodegenerative disease where oxidative stress and mitochondrial dysfunction play important roles in its progression. Tetramethylpyrazine nitrone (TBN), a potent free radical scavenger, has shown protective effects in various neurological conditions. However, the neuroprotective mechanisms of TBN in PD models remain unclear.
Objectives: We aimed to investigate TBN's neuroprotective effects and mechanisms in PD models.
Methods: TBN's neuroprotection was initially measured in MPP^+/MPTP-induced PD models. Subsequently, a luciferase reporter assay was used to detect peroxisome proliferator-activated receptor γ co-activator 1α (PGC-1α) promoter activity. Effects of TBN on antioxidant damage and the PGC-1α/Nuclear factor erythroid-2-related factor 2 (Nrf2) pathway were thoroughly investigated.
Results: In MPP^+-induced cell model, TBN (30–300 μM) increased cell survival by 9.95 % ($P < 0.05$), 16.63 % ($P < 0.001$), and 24.09 % ($P < 0.001$), respectively. TBN enhanced oxidative phosphorylation ($P < 0.05$) and restored PGC-1α transcriptional activity suppressed by MPP^+ (84.30 % *vs* 59.03 %, $P < 0.01$). In MPTP-treated mice, TBN (30 mg/kg) ameliorated motor impairment, increased striatal dopamine levels (16.75 %, $P < 0.001$), dopaminergic neurons survival (27.12 %, $P < 0.001$), and tyrosine hydroxylase expression (28.07 %, $P < 0.01$). Selegiline, a positive control, increased dopamine levels (15.35 %,

* Corresponding authors at: Jinan University College of Pharmacy, 601# Huangpu Road, Guangzhou 510632, China.
E-mail addresses: zaijunzhang@163.com (Z. Zhang), yxy0723@163.com (Y. Sun).
[1] Baojian Guo and Chengyou Zheng contributed equally to this work.

https://doi.org/10.1016/j.jare.2023.11.021

$P < 0.001$) and dopaminergic neurons survival (25.34 %, $P < 0.001$). Additionally, TBN reduced oxidative products and activated the PGC-1α/Nrf2 pathway. PGC-1α knockdown diminished TBN's neuroprotective effects, decreasing cell viability from 73.65 % to 56.87 % ($P < 0.001$).

Conclusion: TBN has demonstrated consistent effectiveness in MPP^+-induced midbrain neurons and MPTP-induced mice. Notably, the therapeutic effect of TBN in mitigating motor deficits and neurodegeneration is superior to selegiline. The neuroprotective mechanisms of TBN are associated with activation of the PGC-1α/Nrf2 pathway, thereby reducing oxidative stress and maintaining mitochondrial function. These findings suggest that TBN may be a promising therapeutic candidate for PD, warranting further development and investigation.

Introduction

Parkinson's disease (PD) is the second most prevalent long-term neurodegenerative disorder. The disease is characterized by both motor and nonmotor manifestations. Motor symptoms are directly associated with the degeneration of dopaminergic neurons in the substantia nigra (SN) [1,2]. Current therapies for PD include dopamine (DA) precursors, DA receptor agonists, monoamine oxidase inhibitors (MAOIs), catecholamine-O-methyltransferase inhibitors. These DA replacement strategies provide symptomatic relief in PD patients but lack neuroprotective or disease-modifying effects [3]. Although the detailed molecular mechanisms underlying the loss of dopaminergic neurons in PD remain unclear, increasing evidence suggests that oxidative stress and mitochondrial dysfunction play an important role [4]. Past clinical trials focused on targeting specific molecular pathways implicated in PD pathogenesis have yielded disappointing results [5]. Consequently, an alternative and potentially more effective approach is to target co-regulatory molecules that address multiple facets of PD pathogenesis, including oxidative stress and mitochondrial dysfunction.

Peroxisome proliferator-activated receptor γ co-activator 1α (PGC-1α) is a well-known transcriptional co-activator that interacts with nuclear respiratory factors to control the expression of nuclear-encoded mitochondrial proteins. These proteins play a crucial role in controlling mitochondrial biogenesis, respiration, and the antioxidant defense system. In early PD patients, low expression of PGC-1α was found in dopaminergic neurons of SN [6]. Sirtuin 1 (SIRT1) activates PGC-1α by deacetylating lysine residues, thereby promoting the expression of PGC-1α [7]. Consequently, these proteins exhibit neuroprotective effects by enhancing neuronal activity and reducing neuronal sensitivity to neurotoxins [8–10]. Overexpression of PGC-1α or application of small-molecule PGC-1α activators can improve mitochondrial function and protect dopaminergic neurons in the MPTP mouse model of PD [6,11–13]. PGC-1α null mice display abnormal mitochondria in neurons and are much more sensitive to oxidative stress. Re-expression of PGC-1α in these mice restores mitochondrial functions and oxidative stress detoxification [14]. Additionally, inhibition of the transcriptional activity and protein expression of PGC-1α leads to alterations in downstream target gene expression, ultimately resulting in structural and functional damage to mitochondria [15]. Taken together, activation of PGC-1α may be a novel strategy to develop mitochondrial-targeted therapy for early intervention in PD.

Nuclear factor erythroid-2-related factor (Nrf2) binds to the antioxidant responsive element (ARE) and exerts an important role in regulating the expression of detoxification genes and oxidative stress-inducible enzymes (e.g., heme oxygenase-1 (HO-1) and NAD(P)H: quinone oxidoreductase-1 (NQO-1)) [16]. Notably, Nrf2 deficiency cooperates in promoting protein aggregation, neuroinflammation, and neuronal death in early-stage PD [17]. Nrf2 overexpression is sufficient to protect against 1-methyl-4-phenyl-1, 2, 3, 6-tetrahydropyridine (MPTP), and modulation of the Nrf2/ARE pathway is a promising target for therapeutics aimed at reducing or preventing neuronal death in PD [16,18]. Studies have also revealed the phosphoinositide 3-kinase (PI3K)/protein kinase B (Akt) pathway can activate Nrf2 by phosphorylating it, while glycogen synthase kinase 3β (GSK-3β) can inhibit Nrf2 by promoting its degradation [19,20]. Targeting Nrf2 may provide a therapeutic option to mitigate oxidative stress-associated PD [21]. PGC-1α co-activation with nuclear respiratory factors 1 (Nrf1) and Nrf2 promotes the expression of antioxidant-responsive genes, and regulates mitochondrial transcription factor A (TFAM) expression, which plays an important role in mtDNA replication, maintenance, and transcription [6]. These findings strongly suggest that PGC-1α/Nrf2 might be a co-regulatory molecule in anti-oxidative stress and improvement of mitochondrial dysfunction to combat PD.

Dysregulation of myocyte enhancer factor 2D (MEF2D) is implicated in the pathogenic process of PD, which is involved in oxidative stress-induced mitochondrial damage and neuronal death [22]. Our previous studies have proved that loss of MEF2D function was associated with increased vulnerability to MPTP- and 6-OHDA-induced toxicity [23–25]. Prior work had suggested that PGC-1α and MEF2 were functionally linked [26]. An isogenic human iPSC PD model shows nitrosative stress-induced dysfunction in MEF2-PGC-1α transcription, contributing to mitochondrial dysfunction and apoptotic cell death [27]. Additionally, it has been shown that Akt and GSK-3β can lead to an increase in the neuronal survival factor MEF2D in the nucleus [28]. Phosphorylation of MEF2D by GSK-3β (the MEF2D inhibitor) promotes neuronal apoptosis [24,29]. Apart from the Akt/GSK-3β pathway, cyclin-dependent kinase 5 (CDK5) has been proposed to inhibit MEF2D. Increased CDK5 activity promotes the phosphorylation of MEF2D at Ser444, which leads to the destabilization of MEF2D and its activity [30]. Collectively, these studies suggest that MEF2D is involved in the pathogenesis of PD and its dysregulation contributes to mitochondrial dysfunction and cell death.

Our laboratory has synthesized 2- [[(1, 1-dimethylethyl) oxidoimino] methyl]-3, 5, 6- trimethylpyrazine (tetramethylpyrazine nitrone, TBN). TBN is the result of arming one of the most widely clinically used natural products, 2, 3, 5, 6-tetramethylpyrazine (TMP), with a powerful free-radical scavenging nitrone group [31] (Fig. 1A). The nitrone group is the active pharmacophore of disodium 4-[(*tert*-butylimino)-methyl] benzene-1, 3-disulfonate *N*-oxide (NXY-059, or disufenton sodium, Cerovive), once the subject of intense clinical investigation [32]. TMP is the major component of the medicinal plant *Ligusticum wallichii* Franchat (Chuan Xiong), the use of which was first recorded during the Chinese Tang dynasty. TMP and its derivatives are used for the treatment of ischemic stroke in China. TMP protects against neuronal damage in rodent PD models by scavenging free reactive oxidant species [33–37]. NXY-059 exhibits significant neuroprotective activity in neurodegenerative diseases [32,38]; unfortunately, however, NXY-059 failed in Phase III studies for the treatment of ischemic

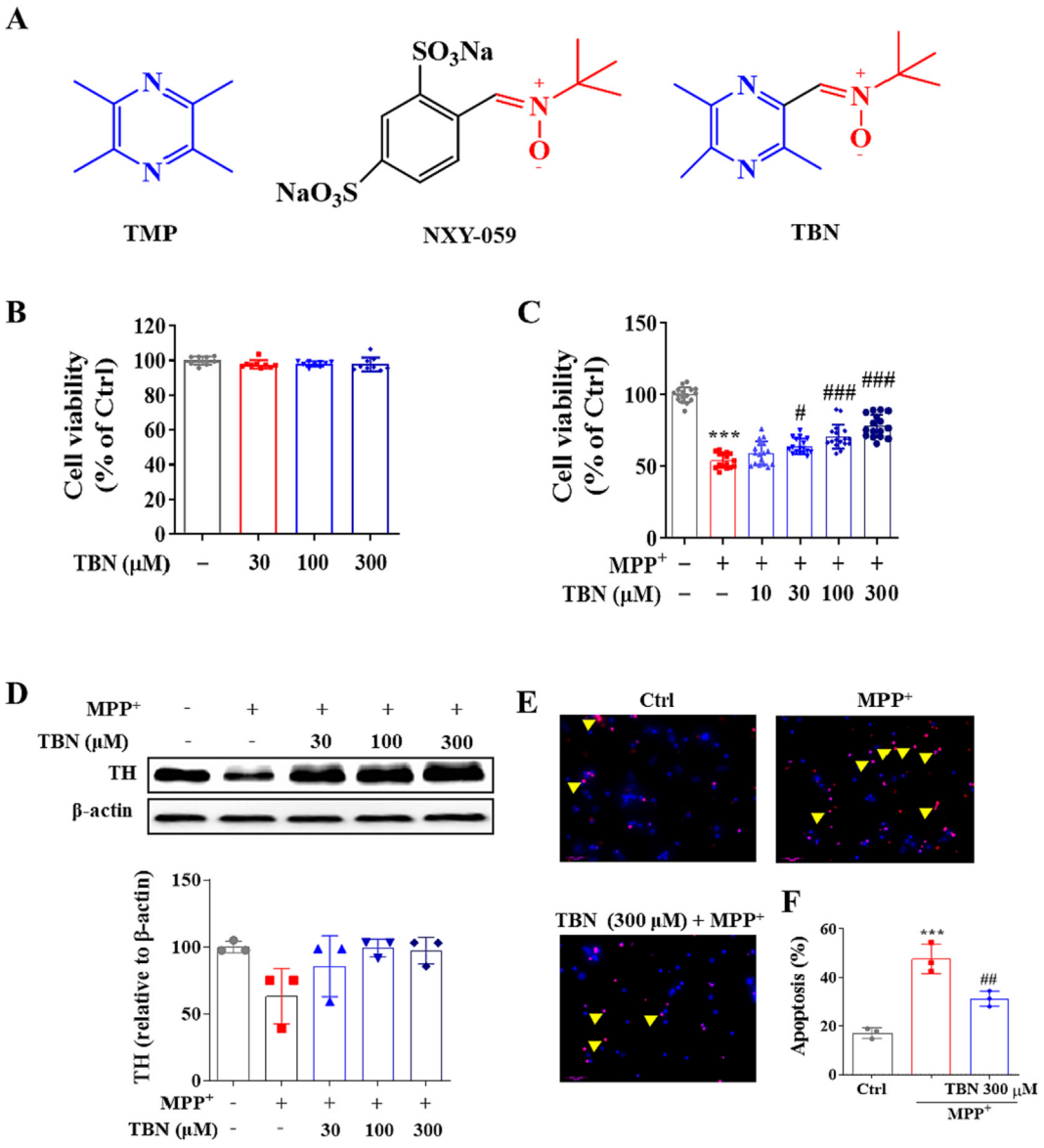

Fig. 1. TBN protects primary midbrain neurons against MPP⁺-induced toxicity. (**A**) Chemical structure of TMP, NXY-059, and TBN. (**B**) TBN has no cytotoxicity on primary midbrain neurons for 24 h incubation at 30–300 μM. Primary midbrain neurons were pre-treated with indicated concentrations of TBN for 2 h followed by treatment with 20 μM MPP^+ for 24 h (**C** and **D**). (**C**) Effect on cell viability of MPP^+-treated neurons. (**D**) Western blot for TH expression in MPP^+-treated neurons. Data are expressed as mean ± SD of three independent experiments. Data were analyzed using Kruskal-Wallis test followed by Dunn's multiple comparisons test (**B**-**D**). CGNs were pre-treated with 300 μM TBN for 2 h followed by 150 μM MPP^+ treatment for 24 h. (**E, F**) Representative graphs and number of apoptotic neurons. Scale bars, 50 μm. Arrows indicate TUNEL-positive cells. Data are expressed as mean ± SD of three random fields. Data were analyzed using one-way ANOVA and Dunnett's multiple comparisons test (**F**). $^{***}P < 0.001$ versus untreated control group. $^{\#}P < 0.05$, $^{\#\#}P < 0.01$ and $^{\#\#\#}P < 0.001$ versus MPP^+ alone group.

stroke because the drug achieved poor penetration of the blood–brain barrier (BBB) in patients [39]. In sharp contrast to NXY-059, TBN efficiently penetrates BBB and delivers the free-radical scavenging nitrone to the brain to provide neuroprotection [40]. Treatment with TBN attenuates apoptotic cell death of primary hippocampal neurons upon deprivation of oxygen and glucose [41]. TBN exhibits significant protective efficacy in preclinical models of ischemic stroke [40–43], subarachnoid hemorrhage, retinopathy [44], and traumatic brain injury [45].

In the present study, we tested the hypothesis that activation of the PGC-1α/Nrf2 signaling pathway by a novel synthetic small molecule TBN could restore the cellular processes that are perturbed in PD and reduce neurodegeneration in cellular and animal models of PD. Thus, we examined TBN for its ability to preserve neuronal viability and mitochondrial function, as well as its capacity to reduce markers of oxidative stress and improve movement disorders in MPTP-induced rodent parkinsonism mice.

Methods and materials

Cell culture and treatment

Rat pheochromocytoma PC12 cells can synthesize DA and norepinephrine and express DA transporters. Neuro-2a (N2a) cells are a fast-growing mouse neuroblastoma cell line with neuronal and amoeboid stem cell morphology. PC12 cells were cultured in DMEM medium (Gibco, Waltham, MA, USA) supplemented with 10 % horse serum (Gibco, Waltham, MA, USA) and 5 % fetal bovine serum (FBS, Gibco, Waltham, MA, USA) in a humidified atmosphere

of 5 % CO_2 and 95 % air at 37 °C. N2a cells were grown in DMEM medium supplemented with 10 % FBS, 100 U/mL penicillin, and 100 μg/mL streptomycin (Gibco, Waltham, MA, USA). After treatment, cells were collected and processed for the dual-luciferase reporter assay, cellular glycolytic function assay, and oxygen consumption assay.

Cerebellar granular neurons (CGNs) were isolated from postnatal 8-day-old Sprague-Dawley rat pups (15–20 g) according to the protocol described previously [46]. Seven days post-culture, CGNs were processed by terminal deoxynucleotidyl transferase (TdT) dUTP nick-end labeling (TUNEL) assay (In situ cell death detection kit, Roche, Mannheim, Germany), MitoCheck mitochondrial complex I activity assay (Cayman Chemical, Ann Arbor, MI. USA), and ATP assay (Beyotime Biotechnology, Nanjing, China).

Primary midbrain neuronal cultures were prepared from the ventral mesencephalon dissected from the embryos of E14 pregnant Sprague-Dawley rats (Animal care facility of SUN YAT-SEN University, Guangzhou, China) as described previously [47]. Five days post-culture, cells were collected and processed for the 3-(4, 5-Dimethylthiazol-2-yl)-2, 5-Diphenyltetrazolium Bromide (MTT) and Western blot assay, respectively.

MTT assay

The MTT assay was performed according to the specifications of the manufacturer (Cell Proliferation Kit I; Sigma-Aldrich, St. Louis, MO, USA). After treatment, the culture medium was removed, basic medium containing 0.5 mg/mL MTT was then added and incubated at 37 °C and 5 % CO_2 for 4 h. The absorbance (OD value) at 570 nm was measured using a multi-function microplate reader (BioTek Corporation, Winooski, VT, USA). Cell viability was expressed as a percentage of the value of the cells without toxin treatment.

Cellular glycolytic function and oxygen consumption

Cellular glycolytic function and oxygen consumption were monitored according to the manufacturer's protocol (Agilent Cell Analysis Technology, Santa Clara, CA, USA) using the Seahorse XF24 analyzer as previously described [48]. PC12 cells were seeded in Seahorse XF 24-well utility plates at a concentration of 2.5×10^5 cells/mL (100 μL/well) and were cultured for 24 h. The cells were then incubated with the indicated TBN concentration with or without 2 mM MPP^+ for 24 h. The extracellular acidification rate (ECAR) and oxygen consumption rate (OCR) parameter values were measured at the indicated time after automatic injection of load compounds in the corresponding well from the appropriate ports of a hydrated sensor cartridge into the identical assay medium. Mitochondrial function parameters were automatically calculated by the Seahorse XF Glycolysis Stress or Mito Stress Test Report Generator.

TUNEL staining

The Click-iT™ plus TUNEL assay was used to detect the apoptotic cells following the recommendations from the supplier. Briefly, CGNs were fixed in 4 % paraformaldehyde (PFA) for 1 h at room temperature and were then incubated in permeabilization solution with freshly prepared 0.1 % Triton X-100 in 0.1 % sodium citrate for 2 min at 4 °C. DNA strand breaks were identified by labeling free 3-OH terminals with modified nucleotides in the TUNEL reaction mixture for 1 h at 37 °C in the dark. The cell nuclei were counterstained with DAPI for 10 min and were viewed with a laser scanning confocal microscope (Leica TCS SP5, Bensheim, Germany). TUNEL-positive cells (%) were calculated from three random fields under 100x magnification for each treatment group.

Mitochondrial complex I activity

Cellular mitochondria were extracted according to the manufacturer's protocol (Beyotime Biotechnology, Beijing, China). The MitoCheck complex I activity assay (Cayman Chemical, Michigan, USA) was used to test mitochondrial complex I activity. Primary CGNs were pre-treated with TBN (10, 30, and 100 μM) for 2 h followed by 150 μM MPP^+ treatment for 24 h. Then, CGNs were homogenized with mitochondrial separation reagent on ice for 15 min. The precipitate was removed by centrifugation at 600 g for 10 min at 4 °C. The supernatant was centrifuged at 11,000 g for 10 min at 4 °C and then resuspended in an isolation buffer. Mitochondrial complex I activity was quantified by measuring the reduction of ubiquinone to ubiquinol following the addition of KCN, NADH, and ubiquinone in the presence and absence of rotenone. The OD value was immediately measured at 340 nm in a multi-function microplate reader. Mitochondrial complex I activity was expressed as a percentage of the value of the cells without inducer treatment.

ATP determination

ATP levels were determined using a luminescent solution (ATP Determination Kit, Beyotime Biotechnology) according to the manufacturer's protocol. Primary CGNs were pre-treated with TBN (10, 30, and 100 μM) for 2 h followed by 150 μM MPP^+ treatment for 24 h. Then, CGNs were homogenized with lysis buffer at 12,000 g for 5 min at 4 °C. The supernatant was collected and protein concentration was quantitated by BCA assay (Pierce Biotechnology, Rockford, IL, USA). Luminescence values were measured on a multi-function microplate reader following the addition of ATP detection reagents. The ATP luminescence (nmol) was determined using a standard curve and was normalized to total protein content (mg) measured by BCA assay.

Luciferase reporter assay of PGC-1α promoter activity

The PGC-1α Dual-Luciferase® Reporter (DLR™) assay (Promega, Fitchburg, WI, USA) was carried out as described previously [49]. N2a cells were transiently transfected with 200 ng renilla luciferase-expressing plasmid (pRL-TK, Promega, Madison, WI), 500 ng PGC-1α-2 kb, 500 ng PGC-1α-ΔCRE or 500 ng PGC-1α-ΔMEF plasmid purchased from Addgene (Watertown, Massachusetts, USA) using Lipofectamine® 3000 (Invitrogen, Carlsbad, CA, USA) for 48 h according to the manufacturer's instructions. The pRL-TK plasmid was used as an internal control. Then, cells were pre-treated with 300 μM TBN for 2 h, followed by 2.5 mM MPP^+ treatment for 24 h. The firefly luciferase luminescence and renilla luciferase activity were measured using a multi-function microplate reader at 0.5 s integration and from the bottom of the plate, respectively. Luciferase values were normalized to the internal control renilla.

Ethics statement

C57BL/6j mice (10–12 weeks old, male mice: 25 ± 1 g weight, female mice: 19 ± 1 g weight, No.44007200009668 and No.44007200012137) were purchased from Guangdong Medical Laboratory Animal Center (Guangzhou, China). Animals were housed 3 to 5 per cage with *ad libitum* access to water and food during a 12 h light/dark cycle. All animal studies were conducted according to the guidelines of the Experimental Animal Care and Use Committee of Jinan University (Guangzhou, China). The experimental protocols were approved by the Ethics Committee for Animal Experiments of Jinan University (20140506103421).

MPTP mice model

Following our previously published procedure [50], MPTP (30 mg/kg) was administered intraperitoneally (i.p.) once daily for 5 consecutive days to induce experimental Parkinsonism. The control group received an equivalent volume of normal saline. To allow for the full conversion of MPTP to its active neurotoxic metabolite MPP^+, a further 3 days were allowed before drug administration. On day 9, TBN (10, 30, and 90 mg/kg), selegiline (10 mg/kg), or an equal volume of saline was administered orally by gavage twice daily for 14 consecutive days.

Footprint test

Before testing, animals were trained for 3 consecutive days. Each animal conducted 3 successive trials each time, with 1 h intervals. The average value was calculated for statistical analysis. A footprint test was used to detect gait abnormalities. The mice were placed in a corridor that was 5 cm wide, 5 cm high, and 85 cm long. The floor of this corridor was covered with white paper. After 2 weeks of TBN treatment in the MPTP-induced mice PD model, the hind paws of each mouse were colored with black dye, and the animal was then placed in the corridor. The total number of footsteps was recorded and the average stride length (cm) was calculated. Additionally, the time (s) taken for the mouse to cross the wooden corridor was recorded.

Electrochemical HPLC analysis for striatal DA, DOPAC, and HVA

The concentrations of DA, 3, 4-dihydroxyphenyl acetic acid (DOPAC), and homovanilic acid (HVA) in the striatum were examined using reverse-phase HPLC with an electrochemical detector (HPLC-ECD) as previously described [51]. Briefly, striatal tissues were promptly dissected on ice, immediately frozen in liquid nitrogen, and subsequently stored at −80 °C until further biochemical assessment. The striatum tissue was weighed, sonicated in 0.1 N perchloric acid (v/w = 10:1), and homogenized by centrifuging at 12,000 g for 20 min at 4 °C. The supernatant was collected, and 20 μL samples were injected into an HPLC-ECD system equipped with an Agilent Eclipse Plus C18 reverse-phase column (4.6 × 150 mm). The mobile phase composition was composed of 50 mM NaH_2PO_4, 0.03 mM EDTA, 0.8 mM sodium octyl sulfate, and 30 mL/L methanol (pH 3.5). A flow rate of 1 mL/min was maintained throughout the analysis. The concentrations of DA and its main metabolite were quantified by extrapolating the peak area from a standard curve constructed under identical conditions. The levels of DA and its main metabolite were expressed as ng/mg tissue weight.

PURE Prep nuclei assay

Nuclear and cytosolic fractions were separated from SN tissue using the PURE Prep Nuclei assay kit (Sigma-Aldrich, St. Louis, MO, USA) in accordance with the manufacturer's protocol. Nuclear and cytosolic fractions were analyzed by Western blot**.**

Western blot

Samples were homogenized with RIPA lysis buffer supplemented with 1 mM PMSF (Sigma-Aldrich, St. Louis, MO, USA) and 1 % (v/v) halt™ phosphatase inhibitor cocktail (100X, Thermo Fisher Scientific, MA, USA) on ice. The precipitate was removed by centrifugation at 12,000g for 30 min at 4 °C. The total protein concentration of the supernatant was determined using the BCA protein assay kit. Subsequently, 30 μg of protein samples were separated by 10–15 % (w/v) SDS-PAGE and transferred onto PVDF membranes. The membranes were blocked with 5 % (w/v) bovine serum albumin in TBST at room temperature for 2 h. The membranes were then incubated with appropriate primary antibodies overnight at 4 °C and were then incubated with HRP-conjugated secondary antibodies in TBST (1:2000 dilution, Cell Signaling Technology, Danvers, MA, USA) for 2 h at room temperature. After incubation with secondary antibodies, the reaction product in the membrane was visualized using an ECL advanced Western blot detection kit (Amersham, Little Chalfont, UK). Western blot images and band densities were captured and quantitatively analyzed using the Care Stream Molecular Imaging Software (Carestream Health Inc, New Haven, CT). Beta-actin or Lamin A/C was used as the loading control, respectively. All primary antibodies used in this study are listed in Table 1.

Immunochemistry or immunofluorescence

Mice in each group were deeply anesthetized with pentobarbital sodium (100 mg/kg, i.p.) and then underwent transcardial perfusion with blood vessel flushing fluid solution (4 % (w/v) PFA in 0.1 M PBS, pH 7.4). The brains were removed and post-fixed for 48 h. The brains were then placed in graded 10 % to 30 % (w/v) sucrose solution in 0.1 M PBS, pH 7.4 for 6 days at 4 °C. Brains were embedded in OCT (Tissue-Tek, Miles Inc., Elkhart, IN), and finally sectioned into 25 μm. Sections were incubated with 3 % (v/v) hydrogen peroxide (H_2O_2) for 15 min at room temperature to inactivate endogenous peroxidase activity followed by antigen retrieval in sodium citrate buffer (10 mM, pH 6.0) for 15 min at 95 °C. Afterward, brain sections were incubated with appropriate primary antibodies overnight at 4 °C. Then, the sections were incubated with appropriate secondary antibodies for 2 h at room temperature. The secondary antibodies were HRP-linked goat-anti-rabbit antibody (1:200 dilution, Cell Signaling Technology, Danvers, MA, USA), Alexa Fluor® 546-conjugated goat anti-rabbit or mouse (1:200 dilution, Invitrogen, Carlsbad, CA, USA) and Alexa Fluor® 488-conjugated goat anti-rabbit or mouse (1:200 dilution, Invitrogen, Carlsbad, CA, USA). Cell nuclei were counterstained with DAPI for 10 min. Immunohistochemistry (TH-stained sections) was revealed using diaminobenzidine (DAB). Stained tissue slides were viewed with a laser scanning confocal microscope (Leica TCS SP5, Bensheim, Germany). The TH-positive cells in SN were counted using the optical fractionator method as described previously [52]. Three randomly selected amplifying fields in each section were chosen to conduct a semi-quantitative analysis using Image-Pro Plus 6.0 software (Media Cybernetics, Silver Spring, USA) in the SN or TH-immuno-reactive neurons. The mean fluorescence densities of 8-OHdG, 4-HNE, 3-NT, MEF2D, and PGC-1α expression levels were subsequently calculated. All primary antibodies used in this study are listed in Table 1.

Total RNA extraction and qRT-PCR

RNA was extracted from the SN using Trizol reagent (Thermo Fisher Scientific, USA). Total RNA (2 μg) was reversely transcribed using M−MuLv Reverse Transcriptase (New England Biolabs, Beverly, MA, USA). Quantitative PCRs were performed in triplicates for all samples using the Mx 3005P Real-Time PCR system (Stratagene) with SYBR Green Supermix (Thermo Fisher Scientific, USA). The reaction condition consisted of an initial denaturation step at 98 °C for 30 s, followed by 40 cycles of 98 °C for 10 s, 60 °C for 30 s, and 72 °C for 15 s in 20 μL reaction volumes. For normalization, ΔC_t values were calculated relative to the levels of 18S rRNA transcripts. All primers for qRT-PCR were validated based on the melting curve and C_t value before use. All mouse primer sequences used in this study are listed in Table 2.

Table 1
Information about primary antibodies used.

Antibody	Species Raised	Isotype	Application, dilution	Catalog number	Source
TH	Rabbit polyclonal	IgG	WB, 1:1000 IHC/IF, 1:500	T8700	Sigma-Aldrich
TH	Mouse monoclonal	IgG1κ	IHC/IF, 1:200	MAB318	Millipore
Phospho-Akt (Ser 473)	Rabbit monoclonal	IgG	WB, 1:1000	4060S	CST
Akt	Rabbit monoclonal	IgG	WB, 1:1000	4691S	CST
Phospho-GSK-3β (Ser 9)	Rabbit monoclonal	IgG	WB, 1:1000	9322S	CST
GSK-3β	Rabbit monoclonal	IgG	WB, 1:1000	12456S	CST
CDK5	Rabbit monoclonal	IgG	WB, 1:1000	14145S	CST
Nrf2	Rabbit polyclonal	IgG	WB, 1:1000 IF, 1:200	SAB4501984	Sigma-Aldrich
MEF2D	Mouse monoclonal	IgG3	WB, 1:500 IF, 1:200	sc-271153	Santa Cruz
SIRT1	Mouse monoclonal	IgG1	WB, 1:1000	8469S	CST
PGC-1α	Rabbit Polyclonal	IgG	WB, 1:500 IF, 1:50	PA5-38022	Invitrogen
PGC-1α	Rabbit polyclonal	IgG	IF, 1:250	HPA063136	Atlas
TFAM	Rabbit monoclonal	IgG	WB, 1:1000	8076S	CST
HO-1	Rabbit monoclonal	IgG	WB, 1:1000	43966S	CST
8-OHdG	Rabbit polyclonal	IgG	IF, 1:250	orb16710	Biorbyt
4-HNE	Mouse monoclonal	IgG	IF, 1:200	SMC-511D-A594	StressMarq
3-NT	Mouse monoclonal	IgG	IF, 1:200	SMC-154D-STR	StressMarq
Lamin A/C	Mouse monoclonal	IgG2a	WB, 1:1000	4777S	CST
β-actin	Rabbit monoclonal	IgG	WB, 1:1000	4970S	CST

Abbreviations: WB: Western blot; IF: Immunofluorescence; IHC: Immunohistochemistry; ICC: Immunocytochemistry; CST: Cell Signaling Technology.

Table 2
Mouse primer sequence used for qRT-PCR.

Gene	Forward primer (5′-3′)	Reverse primer (5′-3′)
PGC-1α	AGCAGAAAGCAATTGAAGAG	AGGTGTAACGGTAGGTGATG
MEF2D	GCTGCTCAAGTACACCGAGT	TCACAGCCGTTGAAACCCTT
Nrf2	TAGATGACCATGAGTCGCTTGC	GCCAAACTTGCTCCATGTCC
HO-1	CACAGCACTATGTAAAGCGTCT	GTAGCGGGTATATGCGTGGG
TFAM	TGCTCTTCAGGGCCTACTCA	ACCATGGTGGCAAACTGTCT
18s rRNA	GTAACCCGTTGAACCCCATT	CCATCCAATCGGTAGTAGCG

TBN concentration measurement in plasma and rat brains

Sprague-Dawley (SD) rats (n = 6, male: female = 1:1, 200–380 g) were administered a single intragastric dose of TBN (45 mg/kg) and were then euthanized 10 or 30 min later. Plasma and whole-brain homogenates were extracted and TBN's concentrations were measured by LC/mass spectrometry (MS) as previously described [53].

TBN tablet pharmacokinetic assessment in healthy Chinese volunteers

The TBN multiple-ascending-dose (MAD) Phase I study in healthy Chinese volunteers was approved by the Ethics Committee of Haikou People's Hospital in China. Written informed consent was obtained from each subject. The TBN MAD Phase I study has been registered at https://www.chinadrugtrials.org.cn/ (CTR20190583) and conducted following the Good Clinical Practices and the Declaration of National Medical Products Administration (NMPA) of China. Twenty-four healthy Chinese volunteers were divided into two groups, one of which received 600 mg of TBN (n = 12, male: female = 1:1), and the other 1200 mg of TBN (n = 12, male: female = 1:1). Subjects were given the desired amount of TBN in tablet form twice daily (12 h intervals) for seven consecutive days. Blood samples were collected in blood collection tubes with EDTA, centrifuged at 1,500 rpm for 10 min, and the supernatant was transferred into labeled tubes before freezing at −80 ± 10 °C until analysis. TBN's concentrations in serum were measured by HPLC-MS/MS (Waters, Massachusetts, USA).

Statistical analysis

Data analyses were performed with GraphPad Prism software 9.0 (GraphPad, San Diego, CA, USA). Results were expressed as mean ± standard deviation (mean ± SD). Differences with $P < 0.05$ were considered significant. The distribution of data was first examined using the Anderson-Darling test, D'Agostino & Pearson test, and Shapiro-Wilk test. The independent unpaired two-tailed Student's *t*-test was performed to evaluate the differences between two groups if the data fit a normal distribution and variances were similar by F test ($P > 0.05$). If variances differed according to the F test ($P < 0.05$), a two-tailed unpaired Student's *t*-test with Welch's correction was used. When the data did not fit a normal distribution, the Mann-Whitney test was conducted. For multiple group comparisons, one-way or two-way analysis of variance (ANOVA) followed by Tukey's or Dunnett's multiple comparisons test was performed if the data fit a normal distribution and variances were similar by F test ($P > 0.05$). If variances differed according to the F test ($P < 0.05$), the Brown-Forsythe and Welch ANOVA test was used. The Kruskal-Wallis test followed by Dunn's multiple comparisons test was conducted when the data did not fit a normal distribution.

Results

TBN protects cultured primary midbrain neurons

The cytotoxicity of TBN was initially tested in cultured primary midbrain neurons. As shown in Fig. 1B, TBN did not show cytotoxicity at concentrations of 30–300 μM. The relative cell viability of TBN (30 to 300 μM) was 97.78 ± 2.34 %, 98.08 ± 1.46 %, and 97.82 ± 3.93 %, respectively (Fig. 1C). Next, we investigated the neuroprotective effect of TBN on MPP^+-induced neurotoxicity in cultured primary midbrain neurons. Treatment with MPP^+ (20 μM) for 24 h resulted in a dramatic decrease in cell viability (45.92 % decrease, $P < 0.05$) and protein expression of tyrosine hydroxylase (TH), which is a marker of dopaminergic neurons (36.79 % decrease). This suggests that MPP^+ treatment can harm the survival and function of dopaminergic neurons. Interestingly, pre-treatment with

TBN (10 to 300 μM) for 2 h prior to MPP^+ exposure resulted in an increase in cell viability in a concentration-dependent manner. The relative cell viability of TBN (30 to 300 μM) was 64.03 ± 5.23 % ($P < 0.05$), 70.71 ± 8.40 % ($P < 0.001$), and 78.17 ± 7.88 % ($P < 0.001$), respectively (Fig. 1C). In addition, TBN (30 to 300 μM) increased the TH protein expression level, it was not statistically significant (Fig. 1D). TBN (300 μM) treatment significantly mitigated neuronal apoptosis induced by MPP^+, as evidenced by the decrease in TUNEL-positive cells ($P < 0.01$). The apoptosis (%) in the TBN group was 31.32 ± 3.18 %, while the apoptosis (%) in the MPP^+ group was 47.69 ± 6.11 % (Fig. 1E, F). These findings indicated that TBN exerted a neuroprotective effect against MPP^+-induced neurotoxicity, potentially offering a therapeutic avenue for the treatment of PD.

TBN improves mitochondrial function

Next, we assessed the effects of TBN on mitochondrial function by measuring OCR and ECAR in PC12 cells that were either incubated with or without TBN in conjunction with MPP^+. Under basal conditions (Fig. 2A, B), TBN (300 μM) treatment does not affect the ECAR of glycolysis (46.26 ± 7.96), glycolytic capacity (78.99 ± 12.99), and glycolytic reserve (32.73 ± 5.36) compared with the control group (39.05 ± 7.09, 72.27 ± 10.24, and 33.22 ± 5.48, respectively). As shown in Fig. 2C-E, TBN (300 μM) treatment significantly increased the OCR of non-mitochondrial oxygen consumption (72.27 ± 25.67, $P < 0.05$), spare respiratory capacity (178.4 ± 48.60 %, $P < 0.01$), coupling efficiency (74.90 ± 7.09 %, $P < 0.001$), basal respiration (120.80 ± 56.02, $P < 0.01$), maximal respiratory capacity (235.90 ± 132.10, $P < 0.01$), and ATP production (91.63 ± 42.24, $P < 0.01$) compared with the control group (49.38 ± 19.61, 119.7 ± 15.18 %, 59.55 ± 8.47 %, 48.72 ± 21.05, 60.27 ± 30.30, and 29.93 ± 13.51, respectively). Under the MPP^+-stressed condition (Fig. 2F, G), MPP^+ caused a decrease in basal respiration, maximal respiratory capacity, and ATP production ($P < 0.01$). However, TBN (300 μM) treatment significantly restored these parameters to levels comparable to those observed in the control group. Specifically, after TBN treatment, basal respiration increased from 199.80 ± 51.83 to 245.10 ± 54.81, maximal respiratory capacity increased from 341.80 ± 120.30 to 465.90 ± 142.60 ($P < 0.05$), and ATP production increased from 138.70 ± 56.31 to 191.90 ± 56.76 ($P < 0.05$). TBN also increased the ATP content in MPP^+-treated primary CGNs in a concentration-dependent manner ($P < 0.001$). Specifically, the results indicated that treatment with 30 μM TBN led to a 27.50 % increase in ATP content, while treatment with 100 μM TBN resulted in a 36.78 % increase (Fig. 2H). Moreover, TBN treatment at concentrations of 30 and 100 μM increased mitochondrial complex I activity by 27.23 % ($P < 0.05$) and 35.64 % ($P < 0.01$), respectively (Fig. 2I). Collectively, these findings suggested that TBN enhanced cellular mitochondrial metabolism through oxidative phosphorylation (OxPhos) but not glycolysis.

TBN activates MEF2D/PGC-1α signaling pathway in MPP^+-induced neurotoxicity

We further investigated the effects of TBN on the expression of MEF2D, SIRT1, and PGC-1α, all of which contribute to neuronal survival. As shown in Fig. 3A and B, TBN treatment increased protein expression of MEF2D, SIRT1, and PGC-1α in a concentration-dependent manner. Specifically, the results showed that TBN treatment at 30, 100, and 300 μM increased MEF2D protein expression by 18.86 %, 48.72 %, and 60.50 % ($P < 0.05$), respectively (Fig. 3B). Similarly, TBN treatment increased SIRT1 protein expression by 47.04 %, 85.28 % ($P < 0.01$), and 100.66 % ($P < 0.001$), respectively (Fig. 3B). Additionally, TBN treatment increased PGC-1α protein expression by 28.07 %, 37.37 %, and 43.33 %, respectively (Fig. 3B). By contrast, PGC-1α siRNA resulted in a 91.4 % decrease (data not shown) in PGC-1α levels and abolished the neuroprotective effect of TBN. The relative cell viability in MPP^+ + TBN (300 μM) group, MPP^+ + TBN (300 μM) + Scrambled siRNA group, and MPP^+ + TBN (300 μM) + PGC-1α siRNA group was 72.85 ± 4.49 %, 73.65 ± 5.03 %, and 56.87 ± 6.62 %, respectively (Fig. 3C). The results demonstrated that PGC-1α was involved in the ability of TBN to protect against neuronal cell death induced by MPP^+. Furthermore, TBN significantly increased the basal transcriptional activity of PGC-1α in N2a cells transfected with a PGC-1α promoter-driven luciferase reporter plasmid ($P < 0.01$, Fig. 3D, E). The relative luciferase activity was 142.09 ± 14.72 % compared to a baseline value of 100.00 ± 5.41 %, indicating that TBN enhanced the normal transcriptional activity of PGC-1α. Moreover, TBN restored the MPP^+-suppressed transcriptional activity of PGC-1α to 84.30 ± 8.22 % compared to the control group (100 %), while MPP^+ treatment reduced it to 59.03 ± 6.22 %, indicating that TBN was able to counteract the negative effect of MPP^+ on the transcriptional activity of PGC-1α. Deletion of the MEF site (PGC-1α-ΔMEF) and the cAMP-response element (CRE) site (PGC-1α-ΔCRE) of the PGC-1α promoter resulted in decreased basal promoter activity by 38.21 % and 33.57 %, suggesting that the activation of PGC-1α by TBN is CRE- and MEF-dependent. These data implied that the neuroprotective effect of TBN depends on the activation of MEF2D/PGC-1α signaling pathway.

TBN exerts neuroprotective effects in the MPTP-induced mice PD model

To determine whether TBN was neuroprotective in animal models of PD, we firstly examined the effects of TBN on motor behavior and neurodegeneration in the MPTP-induced mice model. On the third day after the last MPTP injection, TBN (10, 30, and 90 mg/kg) or an equal volume of saline was administered orally by gavage twice daily for 14 days (Fig. 4A). At day 22, the body weight in all groups have no significant difference (Fig. 4B). The gait abnormalities of mice in the footprint test were reported to be highly correlated with striatal DA content. MPTP injections caused significant impairment of locomotion. Specifically, the MPTP group exhibited an increased time to cross the corridor (6.52 ± 0.88 s, $P < 0.05$) compared to the Sham group (5.53 ± 0.78 s). Additionally, the MPTP group had a decreased stride length (6.06 ± 0.61 cm) compared to the Sham group (6.50 ± 0.69 cm). However, TBN at doses of 30 and 90 mg/kg and selegiline, the positive control drug, attenuated these locomotion impairments (Fig. 4C, D), but the effects were not statistically significant. The brain content (ng/mg striatal tissue) of striatal DA and its metabolites and the number of TH-positive neurons were examined. As expected, MPTP treatment depleted striatal DA (4.25 ± 0.41, $P < 0.001$) and its metabolites DOPAC (0.18 ± 0.05, $P < 0.001$), and HVA (0.36 ± 0.20, $P < 0.01$) compared to the control group (11.83 ± 1.19, 0.49 ± 0.10, and 0.94 ± 0.38, respectively). MPTP treatment also resulted in a reduction in the number of TH-positive neurons, with a decrease of approximately 25.34 % ($P < 0.001$). Additionally, MPTP treatment resulted in a significant decrease in TH expression in the SN, with a reduction of 28.69 % ($P < 0.01$). However, TBN treatment attenuated these MPTP toxic effects (Fig. 4E-K). Collectively, these results demonstrated that TBN decreased MPTP-induced motor behavioral deficits and neurodegeneration.

TBN decreases oxidative damage products in SN of MPTP-induced mice

MPP^+ can be sequestered into synaptosomal vesicles, or concentrated within the mitochondria of dopaminergic neurons, which leads to reactive oxygen species (ROS) production and results in

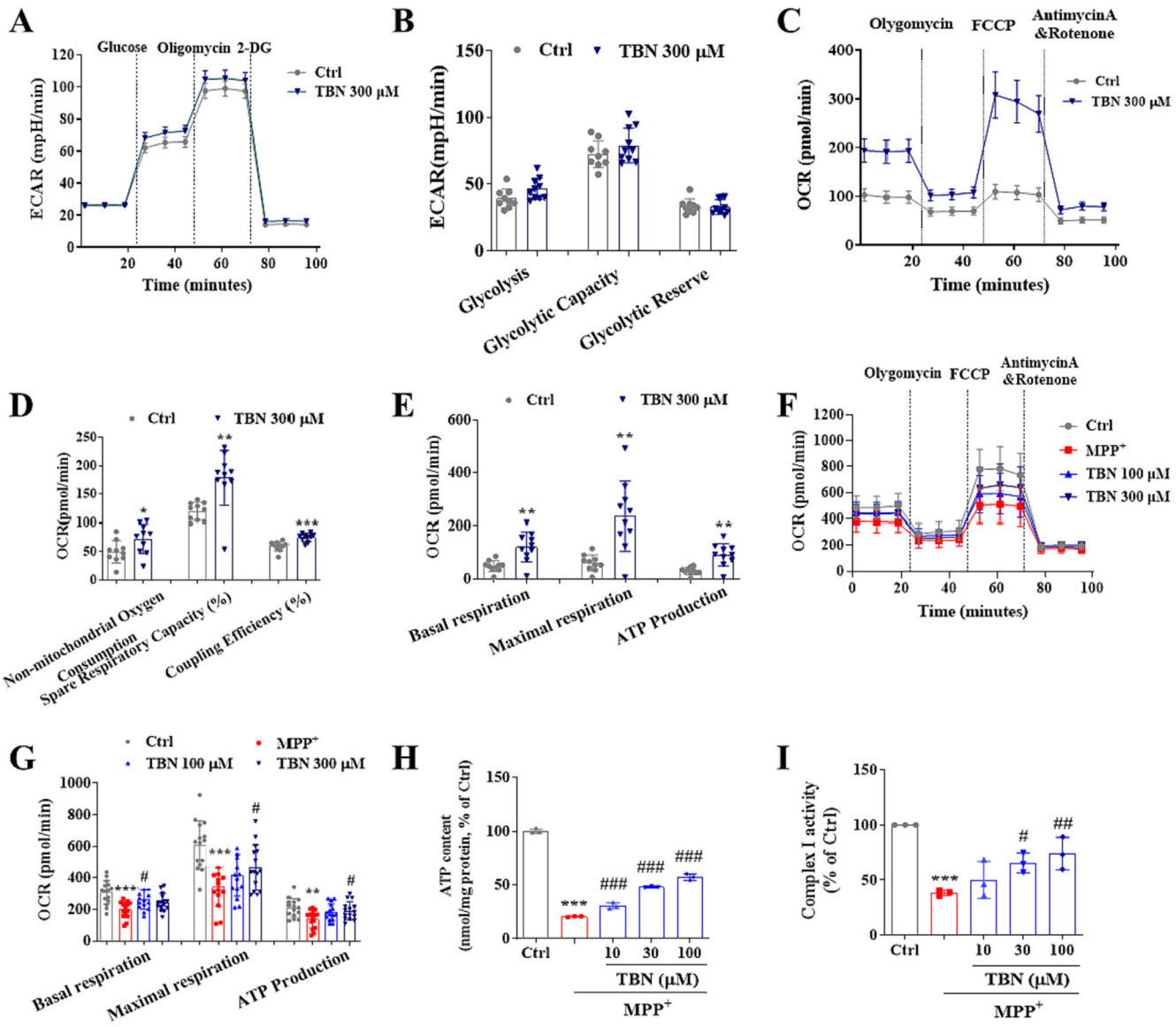

Fig. 2. TBN increases mitochondrial function. (**A**) ECAR response curve. (**B**) Glycolysis, Glycolytic Capacity, and Glycolytic Reserve. (**C**) OCR response curve. **(D)** Non-mitochondrial oxygen consumption, spared respiratory capacity (%), and coupling efficiency (%). Data are mean ± SD of two independent experiments. Data were analyzed using a two-tailed unpaired Student's *t*-test or Mann-Whitney test (**C**, **D**). **(E)** Basal respiration, maximal respiration, and ATP production. Data are mean ± SD of two independent experiments. Data were analyzed using the Mann-Whitney test. (**F**) The response curve of OCR after TBN treatment of MPP^+-induced PC12 cells. (**G**) Basal respiration, maximal respiration, and ATP production. (**H**) ATP content (nmol/mg protein, % of Ctrl). (**I**) Mitochondrial complex I activity (% of Ctrl) in CGNs. Data are mean ± SD of three independent experiments. Data were analyzed using one-way ANOVA followed by Dunnett's multiple comparisons test (**G**-**I**). $^{*}P < 0.05$, $^{**}P < 0.01$ and $^{***}P < 0.001$ versus untreated control group. $^{\#}P < 0.05$, $^{\#\#}P < 0.01$ and $^{\#\#\#}P < 0.001$ versus MPP^+ alone group.

protein oxidation, lipid peroxidation, and DNA oxidative damage. Three-nitrotyrosine (3-NT), 4-hydroxynonenal (4-HNE), and 8-hydroxy-2-deoxyguanosine (8-OHdG) are oxidative products of protein, lipid, and DNA, respectively. Immunofluorescence staining was performed to assess the levels of these oxidative products in the SN. The results showed an increase in the levels of 8-OHdG, 4-HNE, and 3-NT in the SN after MPTP treatment ($P < 0.001$). Specifically, the fluorescence intensity of 8-OHdG, 4-HNE, and 3-NT (expressed as a percentage of the sham group) was 234.4 ± 5.74, 339.50 ± 25.75 %, and 324.60 ± 21.59 %, respectively. In contrast, TBN (30 mg/kg) treatment significantly reduced the levels of these oxidative products. After TBN treatment, the fluorescence intensity of 8-OHdG, 4-HNE, and 3-NT (expressed as a percentage of the sham group) was 166.00 ± 6.84 % ($P < 0.001$), 294.80 ± 16.37 % ($P < 0.05$), and 216.10 ± 8.27 % ($P < 0.001$), respectively (Fig. 5A-D). Taken together, these results demonstrate that TBN protected the animals from the neurotoxic effects of MPTP, as measured by the reduced markers of oxidative damage.

TBN activates PGC-1α/Nrf2 signaling pathway in MPTP-induced mice

The *in vitro* studies showed that TBN protects midbrain neurons by increasing the expression of PGC-1α (Fig. 1 and Fig. 3). Additional studies sought to determine its mechanism of action in neuroprotection in *in vivo* PD models. From Western blot analysis of SN samples from MPTP-treated animals, we found that TBN significantly increased the cytosol protein expression of MEF2D, PGC-1α, Nrf2, HO-1, and TFAM (Fig. 6A, B). Specifically, TBN treatment at 10, 30, and 90 mg/kg increased MEF2D protein expression by 26.07 %, 73.01 %, and 63.61 % ($P < 0.05$), respectively. Similarly, TBN treatment led to an increase in PGC-1α protein expression by 27.07 %, 50.09 % ($P < 0.01$), and 41.32 % ($P < 0.05$), respectively.

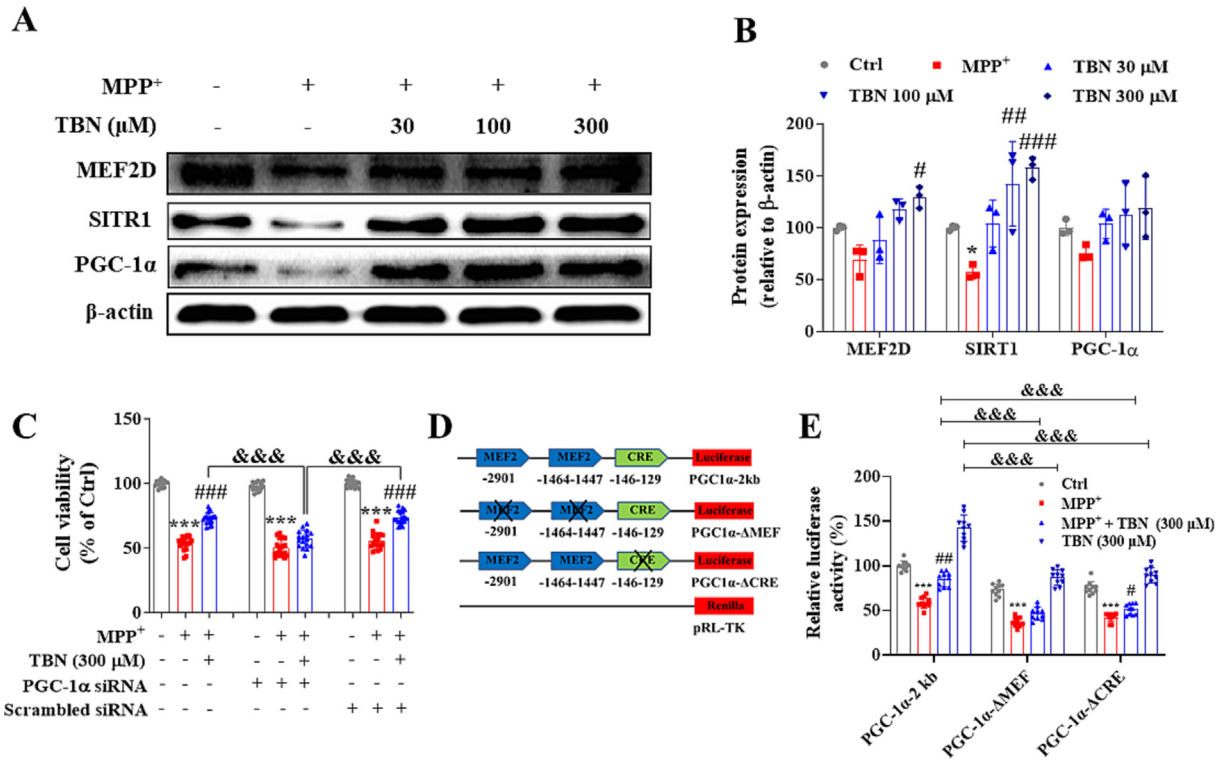

Fig. 3. TBN activates PGC-1α/Nrf2 pathway in MPP$^+$-induced primary midbrain neurons injury. Primary midbrain neurons were pre-treated with indicated concentrations of TBN for 2 h followed by treatment with 20 μM MPP$^+$ for 24 h (A and B). (**A**, **B**) Western blot for expression of MEF2D, SIRT1, and PGC-1α in MPP$^+$-treated neurons. Data are expressed as mean ± SD of three independent experiments. Data were analyzed using Kruskal-Wallis test followed by Dunn's multiple comparisons test (MEF2D) or one-way ANOVA followed by Dunnett's multiple comparisons test (SIRT1 and PGC-1α). (**C**) Silencing of PGC-1α by specific siRNA abolished the protective effect of TBN in MPP$^+$-treated neurons. Data are expressed as mean ± SD of three independent experiments. Data were analyzed using the Brown-Forsythe and Welch ANOVA test. (**D, E**) TBN increased MEF- and CRE-dependent PGC-1α promoter transcriptional activity. Data are expressed as mean ± SD of three independent experiments. Data were analyzed using two-way ANOVA followed by Tukey's multiple comparisons test. $^{*}P < 0.05$ and $^{***}P < 0.001$ versus untreated control group. $^{\#}P < 0.05$, $^{\#\#}P < 0.01$ and $^{\#\#\#}P < 0.001$ versus MPP$^+$ alone group. $^{\&\&\&}P < 0.001$.

Additionally, TBN treatment increased Nrf2 protein expression by 62.41 %, 85.31 %, and 122.61 %, and HO-1 protein expression by 11.28 %, 39.40 % ($P < 0.05$), and 48.64 % ($P < 0.01$), respectively. Furthermore, TBN treatment increased TFAM protein expression by 7.73 %, 31.68 % ($P < 0.01$), and 55.18 % ($P < 0.001$), respectively. Meanwhile, MPTP decreased the nuclear protein levels of MEF2D, PGC-1α, Nrf2, and HO-1, while TBN treatment reversed the changes (Fig. 6C, D). Specifically, TBN treatment at 10, 30, and 90 mg/kg resulted in a respective increase in MEF2D protein expression by 40.96 %, 93.01 % ($P < 0.01$), and 84.81 % ($P < 0.01$), respectively. Similarly, TBN treatment increased PGC-1α protein expression by 33.65 %, 42.21 % ($P < 0.05$), and 50.56 % ($P < 0.01$), respectively. Additionally, TBN treatment increased Nrf2 protein expression by 36.54 %, 45.64 % ($P < 0.05$), and 41.24 % ($P < 0.05$), and HO-1 protein expression by 23.89 %, 25.57 %, and 17.13 %, respectively. To further confirm the effects of TBN on MEF2D or PGC-1α expression in dopaminergic neurons, co-localization analysis of TH with MEF2D or PGC-1α was performed using dual fluorescent immunostaining. The results showed that TBN increased PGC-1α and MEF2D expression in the dopaminergic neurons of MPTP-treated mice ($P < 0.05$, Fig. 6E-H). Specifically, after TBN treatment, the fluorescence intensity of PGC-1α increased from 37.86 % to 62.95 % (expressed as a percentage of the sham group), while the fluorescence intensity of MEF2D increased from 76.31 % to 93.30 % (also expressed as a percentage of the sham group). Furthermore, mRNA expression analysis of SN samples from MPTP-induced model mice revealed that TBN increased the mRNA expression levels of MEF2D ($P < 0.05$), PGC-1α, Nrf2, HO-1 ($P < 0.05$), and TFAM ($P < 0.05$, Fig. 6I-M). Specifically, after TBN treatment, the mRNA levels of MEF2D, PGC-1α, Nrf2, HO-1, and TFAM were 1.57-, 1.62-, 1.53-, 1.87-, and 1.59-fold higher than those of the MPTP group, respectively. Moreover, the upstream signaling pathway of the MEF2D/PGC-1α/Nrf2 pathway was investigated. The results indicated that TBN down-regulated CDK5 and p-GSK-3β expression, and up-regulated p-Akt expression in the brain of MPTP-treated mice (Fig. 7). Specifically, TBN treatment at 10, 30, and 90 mg/kg increased p-Akt protein expression by 84.02 % ($P < 0.01$), 90.02 % ($P < 0.01$), and 54.42 %, respectively. Similarly, TBN treatment increased p-GSK-3β protein expression by 54.42 %, 120.32 % ($P < 0.05$), and 298.82 % ($P < 0.05$), respectively. Additionally, TBN treatment decreased CDK5 protein expression by 83.80 %, 113.90 % ($P < 0.05$), and 125.70 % ($P < 0.05$), respectively. Overall, these findings indicate that TBN exerts its neuroprotective effect by regulating the CDK5 and Akt/GSK-3β pathways, affecting MEF2D activity and ultimately activating the PGC-1α/Nrf2 pathway in the brain of MPTP-treated mice (Fig. 8).

Discussion

Current treatments for PD patients are mainly focused on drugs that replace DA or DA-like substitutes. While these strategies are effective in managing the motor symptoms of PD, they do not have significant neuroprotective effects. Due to the intricate pathophysiology, an innovative approach for PD could involve the development and utilization of multifunctional neuroprotective or neurorestorative drugs, serving as disease-modifying agents. Disease-modifying therapy (DMT) is an intervention that delays

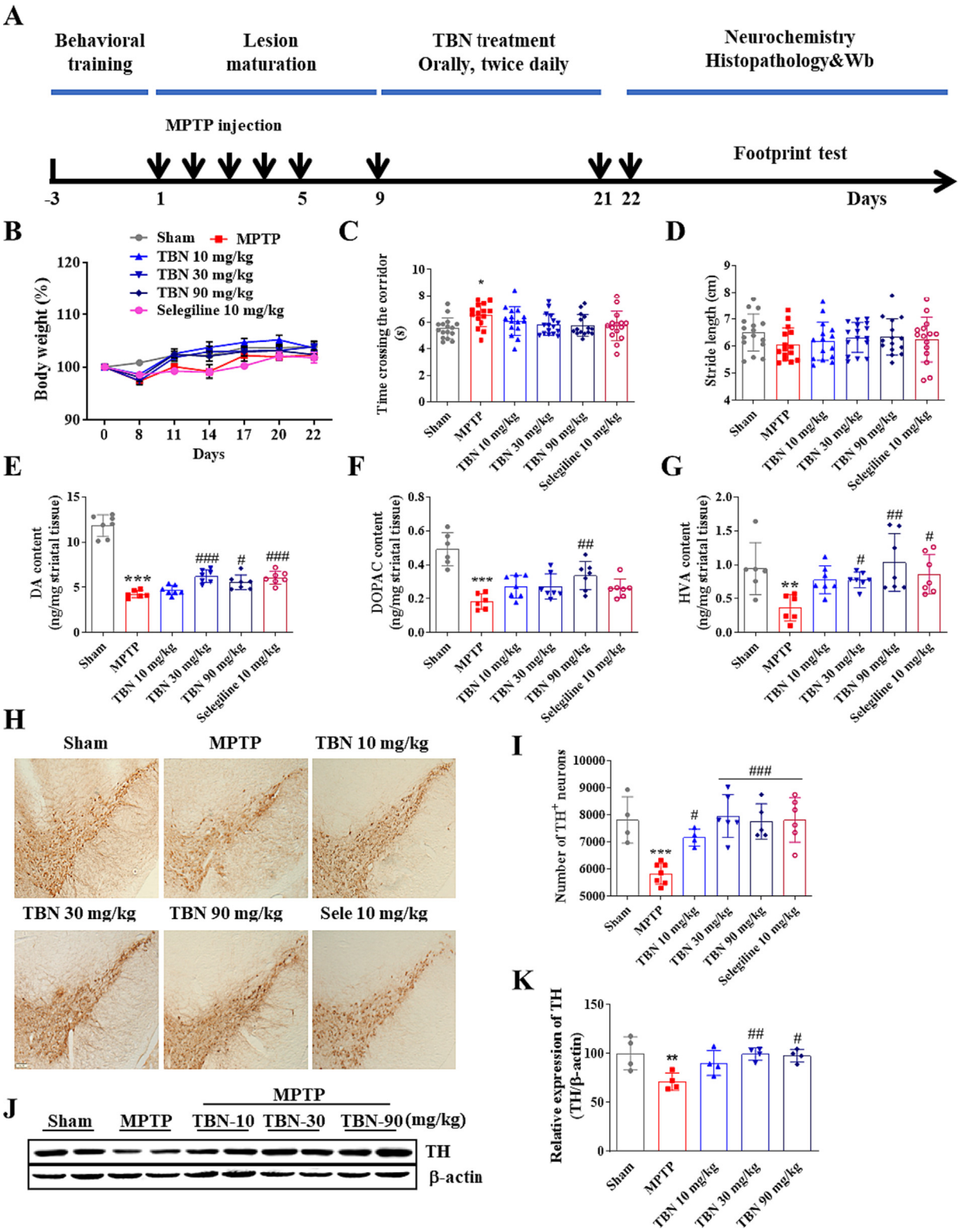

Fig. 4. TBN improves motor behavior and protects SN neurons in the MPTP-induced mice PD model. (**A**) Experimental schedule. (**B**) Body weight (%). Data are mean ± SD of 15 or 16 mice per group. Data were analyzed using two-way ANOVA followed by Tukey's multiple comparisons test. (**C**) Time taken to cross the corridor (s). Data are mean ± SD of 15 or 16 mice per group. Data were analyzed using the Kruskal-Wallis test followed by Dunn's multiple comparisons test. (**D**) Stride length (cm) in the footprint test. Data are mean ± SD of 15 or 16 mice per group. Data were analyzed using one-way ANOVA and Dunnett's multiple comparison tests. (**E-G**) Quantification of striatal DA, DOPAC, and HVA by HPLC. Data are mean ± SD of 6 or 7 mice per group. Data were analyzed using one-way ANOVA followed by Dunnett's multiple comparisons test (E, F) or Kruskal-Wallis test followed by Dunn's multiple comparisons test (G). (**H**) Representative photomicrographs of immunohistochemistry staining for TH in the SN of MPTP mice. Scale bars, 100 μm. (**I**) Stereological counting of TH-positive neurons from SN. (**J, K**) Western blot for TH expression in the SN of MPTP mice. Data are mean ± SD of 4–7 mice per group. Data were analyzed using one-way ANOVA and Dunnett's multiple comparisons test (**I-K**). $^{*}P < 0.05$, $^{**}P < 0.01$ and $^{***}P < 0.001$ versus sham group; $^{\#}P < 0.05$, $^{\#\#}P < 0.01$ and $^{\#\#\#}P < 0.001$ versus MPTP alone group.

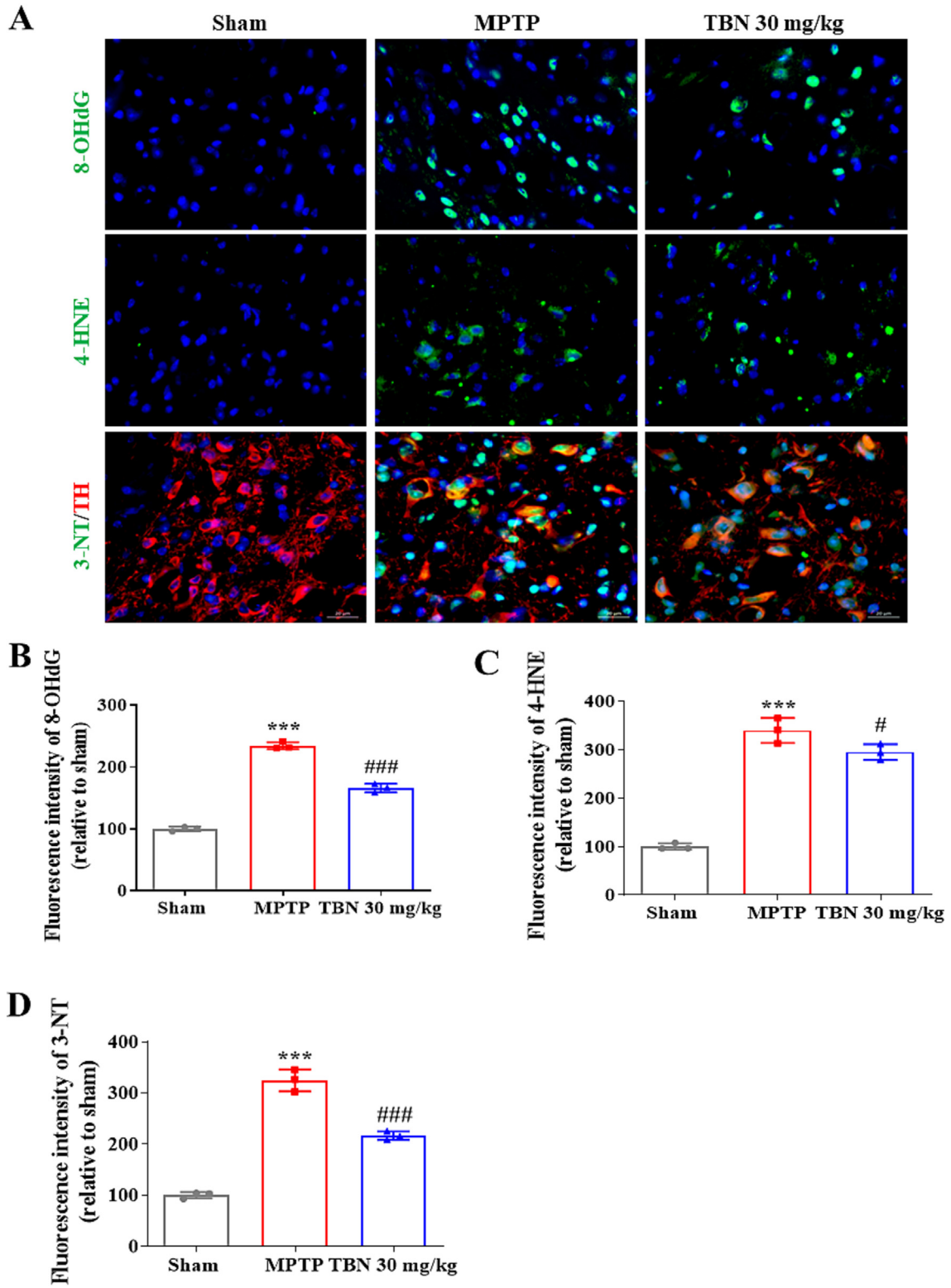

Fig. 5. TBN decreases oxidative damage products in SN of MPTP-induced mice. (**A**) Representative photomicrographs of immunofluorescence staining for 8-OHdG (green), 4-HNE (green), TH (red), 3-NT (green), and Hoechst 33,342 (blue) from SN of MPTP mice. Scale bars, 20 μm. (**B-D**) Fluorescence intensity of 8-OHdG, 4-HNE, and 3-NT in the SN. Data are mean ± SD of 3 mice per group. Three amplifying fields in each section were randomly chosen to conduct a semi-quantitative analysis. Data were analyzed using one-way ANOVA followed by Dunnett's multiple comparisons test. $^{***}P < 0.001$ versus sham group; $^{\#}P < 0.05$ and $^{\#\#\#}P < 0.001$ versus MPTP group. (For interpretation of the references to colour in this figure legend, the reader is referred to the web version of this article.)

or stops neurodegeneration, can affect the initial triggers of neuronal degeneration, prompt neuronal compensatory responses or reduce the spread and progression of pathology. The primary goal of DMT in PD is neuroprotection. Although multiple agents attempting disease modification of PD have been tested in clinical trials, all have failed in the past few decades. The feasibility of

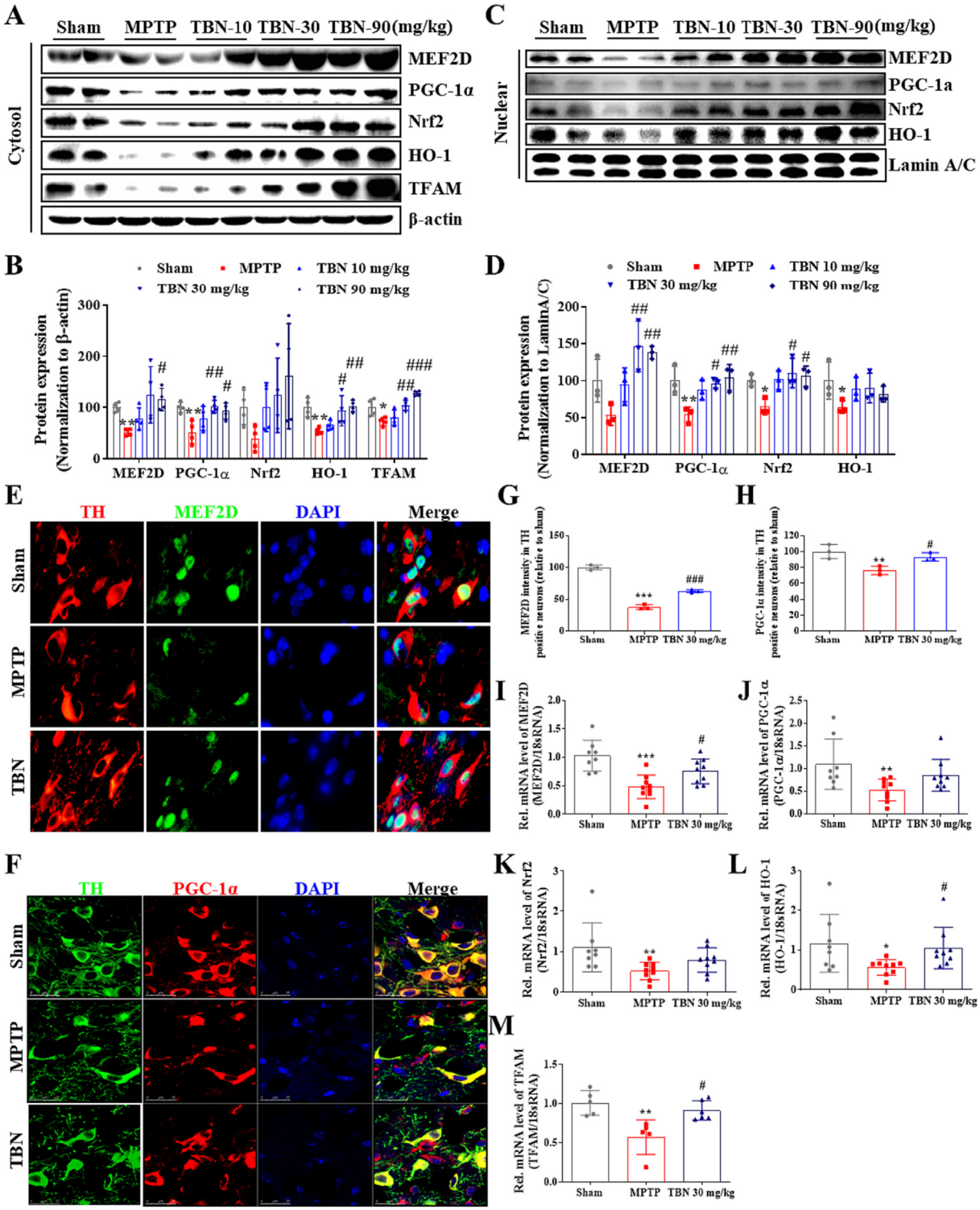

Fig. 6. TBN activates PGC-1α/Nrf2 pathway in MPTP-induced PD mice. (**A, B**) Western blot for expression of MEF2D, PGC-1α, Nrf2, HO-1, and TFAM in the cytosol of SN tissue from MPTP mice. Data were mean ± SD of 4 mice per group. Data were analyzed using one-way Brown-Forsythe and Welch ANOVA test (MEF2D and Nrf2) or ANOVA followed by Dunnett's multiple comparisons test (PGC-1α, HO-1, and TFAM). (**C, D**) Western blot for expression of MEF2D, PGC-1α, Nrf2, and HO-1 in the nuclei of SN tissue from MPTP mice. Data were mean ± SD of 3 mice per group. Data were analyzed using one-way ANOVA followed by Dunnett's multiple comparisons test (MEF2D and PGC-1α) or Kruskal-Wallis test followed by Dunn's multiple comparisons test (Nrf2 and HO-1). (**E**) Representative photomicrographs of co-immunofluorescence staining for TH (red), MEF2D (green), and DAPI (blue). Scale bars, 20 μm. (**F**) Representative photomicrographs of co-immunofluorescence staining for TH (green), PGC-1α (red), and DAPI (blue) in the SN of MPTP mice. Scale bars, 25 μm. (**G, H**) Fluorescence intensity of MEF2D and PGC-1α in the TH-positive neurons. Data were mean ± SD of 3 mice per group. Data were analyzed using one-way ANOVA followed by Dunnett's multiple comparisons test. RNA from SN of PD animals was purified and converted into cDNA, and mRNA expression levels were determined using qRT-PCR. (**I-M**) Relative mRNA expression of (**I**) MEF2D, (**J**) PGC-1α, (**K**) Nrf2, (**L**) HO-1, and (**M**) TFAM in MPTP mice model. Data were mean ± SD of 5–9 mice per group. Data were analyzed using one-way ANOVA followed by Dunnett's multiple comparisons test (I) or Kruskal-Wallis test followed by Dunn's multiple comparisons test (J, K-M). $^{*}P < 0.05$, $^{**}P < 0.01$ and $^{***}P < 0.001$ versus sham group; $^{\#}P < 0.05$, $^{\#\#}P < 0.01$ and $^{\#\#\#}P < 0.001$ versus MPTP group. (For interpretation of the references to colour in this figure legend, the reader is referred to the web version of this article.)

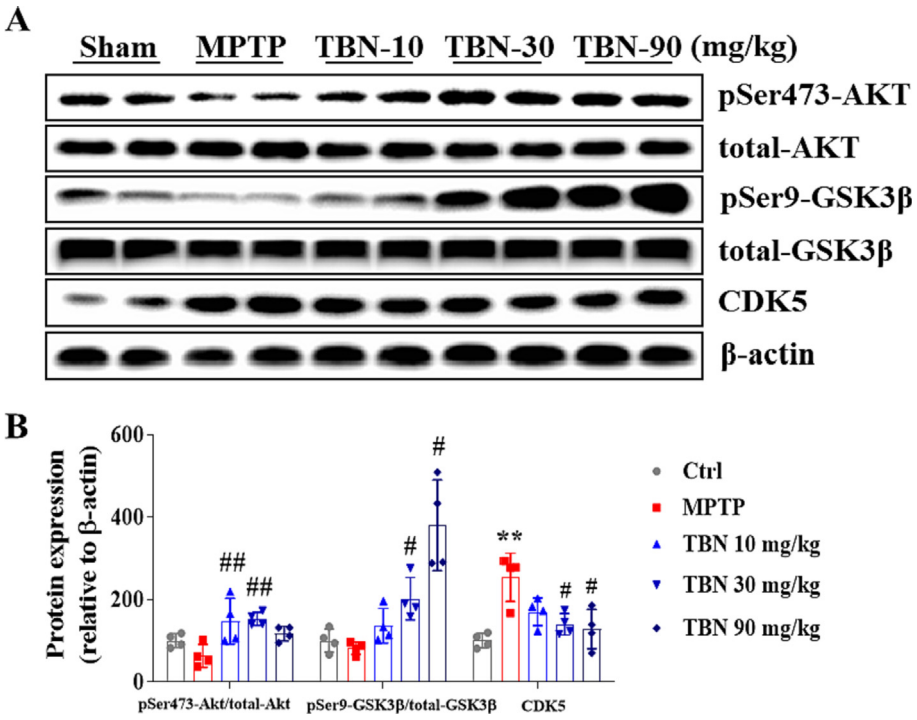

Fig. 7. TBN regulates AKT/GSK3β and CDK5 protein expression in MPTP-induced mice PD model. (**A**, **B**) Western blot showed that TBN increased phosphorylated AKT (Ser 473) and phosphorylated GSK3β (Ser 9), and decreased the expression of CKD5, as compared with the MPTP model group. Data are mean ± SD of 4 mice per group. Data were analyzed using one-way ANOVA followed by Dunnett's multiple comparisons test. $^{**}P < 0.01$ versus sham group; $^{\#}P < 0.05$ and $^{\#\#}P < 0.01$ versus MPTP group.

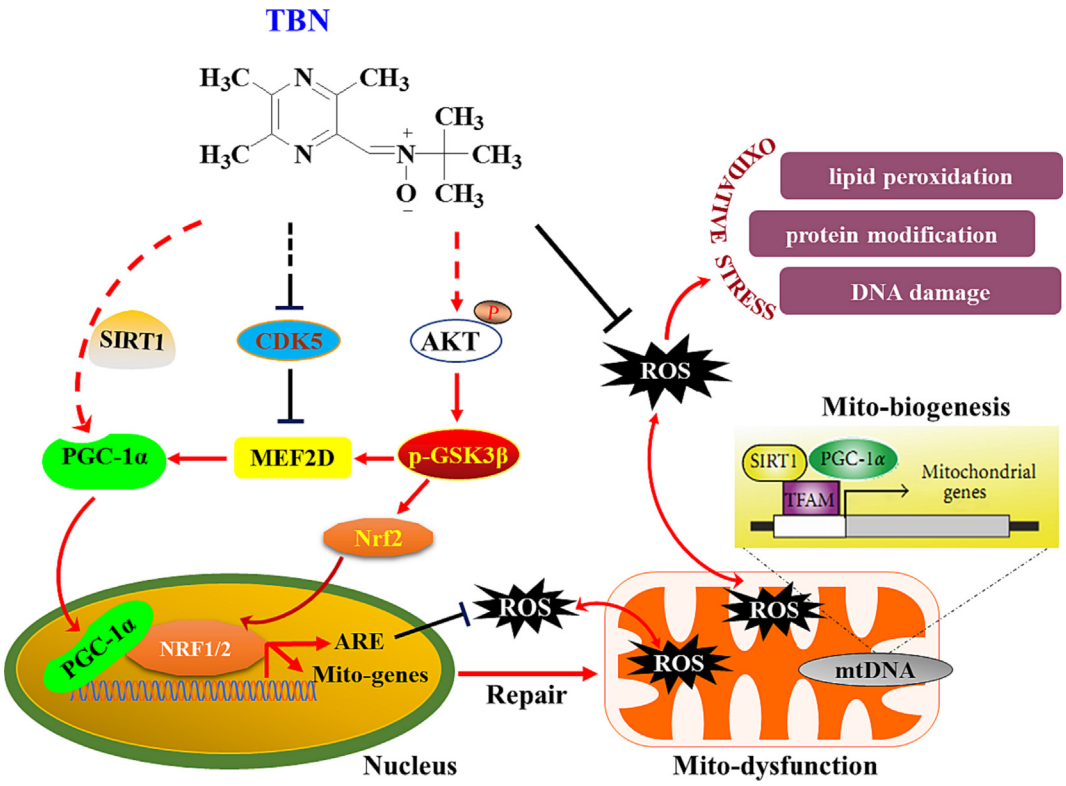

Fig. 8. Schematic diagram of proposed TBN's mechanisms of action in experimental PD models. TBN inhibits CDK5 and activates Akt/GSK-3β pathway. The MEF2/PGC-1α/Nrf2 signaling pathway was then activated, resulting in reduced oxidative stress, and enhanced mitochondrial function, eventually preventing the advance of nigral DA neurodegeneration in experimental models of PD.

moving disease modifying agents to market has been shown through the success of MAO-B inhibitor rasagiline, which has been shown to have neuroprotective or disease modifying activity and has made it to the market as a PD therapeutic. Therefore, DMT that reduces the rate of neurodegeneration or halts disease progress is still one of the greatest unmet needs for PD therapy. TBN is a novel, orally bioavailable, multifunctional neuroprotective agent, which is being developed for the treatment of PD and other diseases. In this study, TBN proved to be consistently effective in MPP^+-induced primary neurons and MPTP-induced mice (Figs. 1 and 4). Notably, TBN was administered after the neurodegenerative process had been initiated by MPTP (3 days after the last dose) intoxication, in which SN dopaminergic neurons continue to die for weeks. Additionally, we found that TBN exhibited neuroprotective effects in 6-OHDA-lesioned PD models, and significantly slowed or even stopped the worsening of motor deficits, apparently modifying the advance of the evolving disease in the hA53T Tg mice (data not shown). The neuroprotective effects of TBN were associated with activation of the PGC-1α/Nrf2 pathway. In summary, our findings suggest that TBN could be a multifunctional neuroprotective candidate for PD disease-modifying treatment, warranting further development and investigation.

MPTP is a neurotoxin that specifically targets and damages SN dopaminergic neurons. However, its time course and pathological features may not fully replicate those seen in human disease. Despite the limitations, current animal models provide a useful platform to selectively study pathophysiology, and the interactions of the multiple etiologic factors involved in PD and help in the development of potential therapeutic strategies for PD. Many early attempts at translating preclinical findings to clinical trial outcomes were still based on the widely used MPTP-induced animal models. In the present study, we found that treatment with MPP^+ resulted in a 45.92 % decrease in cell viability and a 36.79 % decrease in protein expression of TH. In MPTP-induced PD model, MPTP treatment depleted striatal DA by 64.07 % and its metabolites DOPAC by 62.59 %, and HVA by 61.28 %, respectively. Additionally, MPTP resulted in a decrease of approximately 25.34 % in the number of TH-positive neurons and a reduction of 28.69 % in TH expression in the SN. Thus, reduction in the striatal DA and the number of TH-positive neurons in MPTP mice observed in the present study may reflect the actual loss of dopaminergic fibers and neurons. Those changes further led to significant locomotion impairment. TBN's neuroprotective concentration against MPP^+-induced toxicity in cultured primary midbrain neurons ranged from 30 to 300 μM. When the rats were administered a single intragastric dose at 45 mg/kg, the plasma concentrations of TBN were 163.09 μM and 119.13 μM, 10 and 30 min after drug administration, respectively. At the same time, the TBN brain concentrations reached approximately 127.70 μM and 100.08 μM, respectively (assuming the volume of 1 g brain tissue is 1 mL) (Table 3). Most importantly, in the Phase I clinical study, TBN is safe and well-tolerated in healthy Chinese volunteers at 1200 mg/person orally twice daily for 7 days, the TBN maximum serum concentration (C_{max}) reached 114.35 μM (Table 4). These results demonstrate that the TBN effective concentrations shown in *in vitro* and *in vivo* models of PD can be achieved in humans. Selegiline, as an irreversible MAO-B inhibitor, have been developed and prescribed to the patients with PD in clinics. However, several studies still have cast doubt on the efficacy and the long-term balance of benefits and risks. The typical clinical dosage of selegiline in humans ranges from 5 to 10 mg/day (oral). Based on body surface area conversion, assuming an average adult human weight of 70 kg, the equivalent dose of selegiline in mice is approximately 0.65–1.3 mg/kg. In contrast, TBN administered at 10 and 30 mg/kg increased TH-positive neurons by 17.01 % and 27.12 %, respectively, and selegiline administered at 10 mg/kg increased TH-positive neurons by 25.34 %. Therefore, we believe that TBN may be more effective than selegiline. Meanwhile, we cannot exclude the possibility that the effective dose (10 mg/kg) of selegiline in MPTP mice is higher than the therapeutic doses for patients with PD (5–10 mg/day, oral) because of pathological differences between subacute MPTP mice and PD patients. Therefore, further research and clinical trials are necessary to validate these findings and determine the efficacy of TBN for PD treatment.

Although the etiology of PD is complex, mitochondrial dysfunction and oxidative stress remain important steps in the pathogenesis of PD. Agents capable of antioxidation and/or improving mitochondrial function, including coenzyme Q10, creatine, vitamin E, *etc*., have been extensively studied in clinical trials. Although none of these clinical trials have convincingly shown disease-modifying effects, the failure of these drugs does not dismiss the major role of oxidative stress and mitochondrial dysfunction in PD, and thus should not preclude further investigation into upstream pathways to control mitochondrial function and inhibit oxidative stress as potential therapeutic targets. Mitochondrial glycolysis and OxPhos are the primary energy production pathways in cells. Oligomycin, an inhibitor of ATP synthase, inhibits aerobic respiration and stimulates the maximum glycolysis capacity for ATP production. Conversely, 2-DG, a competitive inhibitor of hexokinase, hampers glycolysis and consequently reduces ATP production and cellular metabolic activity. In our study, under basal conditions, treatment with TBN (300 μM) did not alter glycolysis, glycolytic capacity, or glycolytic reserve (Fig. 2A, B), suggesting that TBN may not primarily influence glycolysis for ATP production. Next, we examined the impact of TBN on OCR. Under the basal or MPP^+-stressed condition, TBN at 100 and 300 μM treatment significantly restored basal respiration (Fig. 2E, G), which refers to the minimum level of oxygen consumption required for basic cellular functions in the absence of any specific stimulation. TBN also significantly increased the maximal respiratory capacity (Fig. 2E, G), which refers to the maximum rate at which cells can consume oxygen after FCCP injections. This suggests that TBN may interfere with FCCP, an uncoupling agent disrupting the permeability of the mitochondrial inner membrane. TBN potentially prevents FCCP from destroying the proton gradient across the membrane, uncoupling ATP synthesis from electron transport, consequently raising cellular oxygen consumption to compensate for reduced ATP production. Moreover, under basal conditions, TBN treatment significantly increased the OCR of non-mitochondrial oxygen consumption (Fig. 2D) after Rotenone/Antimycin A injection, suggesting an influence on complex I and III activities. This effect may counteract Rotenone/Antimycin A-induced depression of aerobic respiration and ATP production reduction. Despite the cellular attempt to increase glycolysis when ATP production decreases, TBN did not affect glycolysis, suggesting a potential influence on mitochondrial complex I and III activities. Additionally, TBN significantly increased ATP production after oligomycin injection (Fig. 2E, G). We infer that the reason for this phenomenon is that TBN increases basal oxygen consumption, which can help to compensate for the decrease in ATP production caused by oligomycin. While TBN's potential impact on ATP synthase activity warrants further investigation, subsequent experiments corroborated our Seahorse assay findings. TBN concentration-dependently increased ATP content (Fig. 2H) and mitochondrial complex I activity (Fig. 2I) in MPP^+-treated primary CGNs, reinforcing the notion that TBN enhances mitochondrial OxPhos. This enhancement holds promise as a therapeutic strategy for conditions linked to mitochondrial dysfunction.

What is the possible mechanism of the neuroprotective effects of TBN in PD models? PGC-1α is a transcriptional co-activator that plays a crucial role in various physiological processes, such as energy metabolism, mitochondrial biogenesis, and oxidative stress

Table 3
TBN concentration in the plasma and brain of rats after a single 45 mg/kg intragastric administration.

	Concentration in plasma (ng/mL)		Concentration in the brain (ng/g)	
	10 min	30 min	10 min	30 min
TBN	36043.72	26327.75	28221.59	22117.40

Table 4
TBN pharmacokinetics in healthy Chinese volunteers after multiple-dose administration for 7 days.

	Dose (mg)	$t_{1/2}$ (h)	T_{max} (h)	C_{max} (ng/mL)	C_{min} (ng/mL)	C_{avg} (ng/mL)	CLss/F (ng/mL)	Vss/F (mL/h)	$AUC_{0\text{-}tau}$ (h·ng/mL)
TBN	600	1.89	3.38	9583.79	77.01	1979.82	32593.82	88828.76	23757.87
	1200	2.30	2.56	25271.09	524.03	6775.17	17397.63	57710.15	81302.08

$t_{1/2}$ = elimination half-life; **T_{max}** = time to peak concentration; **C_{max}** = maximum serum concentration; **C_{min}** = steady state trough concentration; **Cavg** = average steady state concentration; **Clss/F** = steady state clearance; **Vss/F** = steady state volume of distribution; **$AUC_{0\text{-}tau}$** = AUC at steady state during one dose interval.

response. SIRT1 is then thought to deacetylate and activate PGC-1α. The overexpression of PGC-1α in several *in vitro* and *in vivo* models results in overall protection against neurodegeneration. However, in MPTP-induced PD model, overexpression of PGC-1α using AAV results in increased vulnerability to the toxin. This may be due to extraordinarily high levels of PGC-1α suppressing the Pitx3/brain-derived neurotrophic factor (BDNF) pathway, which is involved in the development and maintenance of dopaminergic neurons. Encouragingly, we recently found that TBN increased the protein expression of BDNF in a rat model of ischemic stroke, warranting further investigation of the effect of TBN in regulating Pitx3. Therefore, the precise levels of PGC-1α expression and the method of PGC-1α modulation should be given careful attention to achieve its protective potential while avoiding its potentially deleterious effects. In this study, we found that TBN increased protein expression of SIRT1 and PGC-1α in a concentration-dependent manner (Fig. 3A, B). In MPTP-induced PD model, TBN at 30 mg/kg also significantly increased the cytosol and nuclear protein expression of PGC-1α, as well as elevated mRNA levels of PGC-1α (Fig. 6B, D, J). Notably, silencing PGC-1α (using specific siRNA) significantly abolished the neuroprotective effects of TBN *in vitro* (Fig. 3C). PGC-1α co-activation with Nrf1 and Nrf2 promotes the expression of antioxidant-responsive genes, and regulates TFAM expression, which plays an important role in mitochondrial biogenesis. Our present study demonstrated that TBN increased Nrf2, HO-1, and TFAM expression in MPTP-induced PD model (Fig. 6), subsequently improving mitochondrial function (Fig. 2) and reducing markers of oxidative damage, including 8-OHdG, 4-HNE, and 3-NT (Fig. 5). This observation aligns with existing evidence that underscores the pivotal role of PGC-1α/Nrf2 pathway in mediating neuroprotective effects. Collectively, our findings strongly suggest that PGC-1α/Nrf2 pathway likely serves as a key mediator of TBN's neuroprotective effects. However, the direct interaction between TBN and PGC-1α, as well as the specific effects of PGC-1α knockdown on dopaminergic neurons, particularly in MPTP-induced *in vivo* PD models, are still unclear and require further investigation in subsequent studies. By doing so, we can gain a more comprehensive understanding of the intricate interplay between TBN, PGC-1α, and the neuroprotective pathways involved in mitigating PD-associated neurodegeneration. These endeavors would contribute significantly to the elucidation of TBN's therapeutic potential and its precise mechanisms of action in the context of PD.

Additional investigations were conducted to delve deeper into the regulatory mechanisms preceding the PGC-1α/Nrf2 pathway, with a specific emphasis on MEF2D. It has been previously established that enhancing MEF2D can protect SN dopaminergic neurons from toxicity in animal models of PD. In the present study, we found that TBN significantly increased the expression of MEF2D (Fig. 3B; Fig. 6A-D, E, G, I). To further elucidate the role of MEF2D in this context, we conducted experiments involving the deletion of the MEF site from the PGC-1α promoter. The results revealed that PGC-1α-ΔMEF resulted in decreased basal promoter activity and failure to respond to TBN treatment (Fig. 3E). This finding underscores the crucial role of the MEF2D in the regulatory cascade, suggesting its involvement in mediating the protective effects on SN dopaminergic neurons. Moreover, we explored the involvement of key biochemical pathways, such as CDK5, and Akt-GSK-3β, in phosphorylating MEF2D to regulate its activity. Our findings indicated that TBN down-regulated CDK5 expression, and up-regulated p-Akt and p-GSK3β expression (Fig. 7), suggesting a potential pathway through which TBN activates MEF2D. Nevertheless, the direct effect of TBN on CDK5, Akt, and GSK-3β remains unclear, warranting further investigation in future studies. Collectively, the current findings suggest that TBN activates MEF2D through the Akt/GSK3β pathway while inhibiting CDK5 (Fig. 8). These intricate molecular interactions underscore the multifaceted nature of TBN's neuroprotective mechanisms, offering promising avenues for future research.

This study further confirms that activation of the PGC-1α/Nrf2 pathway may improve mitochondrial dysfunction, inhibit oxidative stress, and alleviate the degeneration of SN dopaminergic neurons in PD. However, the limitation of this study is that the exact targets that TBN acts on are not yet clear. We cannot rule out the possibility that TBN may also act through other pathways. Acknowledging these existing limitations, conducting a more thorough evaluation of the mechanisms of action of TBN will establish a robust foundation for devising targeted and efficacious strategies for PD treatment.

Conclusions

Overall, our results demonstrate that TBN is effective in MPP^+-induced cultured primary midbrain neurons at concentrations of 30 and 100 μM. Extending our investigation to the MPTP-induced PD model, TBN administered at a dose of 30 mg/kg exhibits superior neuroprotective effects in mitigating motor behavioral deficits and preventing the neurodegeneration of SN dopaminergic neurons. Moreover, the therapeutic effect of TBN is superior to selegiline. Notably, the effective concentrations of TBN shown in *in vitro* and *in vivo* models of PD can be feasibly achieved in humans. TBN exerts neuroprotection via activation of PGC-1α/Nrf2 pathway, thereby reducing oxidative stress and maintaining mitochondrial function. Additionally, TBN can inhibit CDK5 and activate the Akt/GSK-3β pathway, thereby further regulating the PGC-1α/Nrf2 pathway. Our findings provide valuable insights into the intricate relationship among TBN, the PGC-1α/

Nrf2 pathway, mitochondria dysfunction, and PD. This study serves as a foundational reference for forthcoming clinical trials. Hopefully, TBN is a promising therapeutic candidate to prevent or slow the progress of neurodegeneration in PD.

Ethics approval and consent to participate

All animal studies were conducted according to the guidelines of the Experimental Animal Care and Use Committee of Jinan University (Guangzhou, China). The experimental protocols were approved by the Ethics Committee for Animal Experiments of Jinan University (20140506103421).

CRediT authorship contribution statement

BaojianGuo: Conceptualization, Methodology, Investigation, Software, Formal analysis, Writing - original draft, Funding acquisition. **ChengyouZheng:** Conceptualization, Methodology, Data curation, Validation. **JieCao:** Methodology, Data curation. **FangchengLuo:** Methodology, Data curation. **HaitaoLi:** Conceptualization, Writing – review & editing. **ShengquanHu:** Methodology, Data curation, Funding acquisition. **SimonMingyuan Lee:** Conceptualization, Writing – review & editing. **XifeiYang:** Conceptualization, Writing – review & editing. **GaoxiaoZhang:** Conceptualization, Writing – review & editing. **ZaijunZhang:** Conceptualization, Methodology, Project administration, Writing – original draft, Funding acquisition. **YeweiSun:** Conceptualization, Methodology, Datacuration, Writing – review & editing, Funding acquisition. **YuqiangWang:** Conceptualization, Methodology, Writing – original draft, Funding acquisition.

Declaration of competing interest

The authors declare that they have no known competing financial interests or personal relationships that could have appeared to influence the work reported in this paper.

Acknowledgements

We thank Prof. Spencer Peter for his critical reading and editing of the manuscript. Many thanks also to Linda Wang for editing the manuscript. This work was partially supported by grants from the National Natural Science Foundation of China (NSFC82073821, 82003726, and 81872842), NSFC (31861163001)-Macau Science and Development Fund (FDCT 0004/2018/AFJ) Cooperative Project, the National Innovative Drug Program of China (2018ZX09301009-001), Scientific Projects of Guangdong Province (2021A0505080012, 2020A1515011060, 2020A1515011427, and 2019A1515110751), Science and Technology Projects in Guangzhou (202102070001), Shenzhen Municipal Science and Technology Project (JCYJ20190812171005713).

Appendix A. Supplementary material

Supplementary data to this article can be found online at https://doi.org/10.1016/j.jare.2023.11.021.

References

[1] Costa HN, Esteves AR, Empadinhas N, Cardoso SM. Parkinson's disease: a multisystem disorder. Neurosci Bull 2023;39:113–24. doi: https://doi.org/10.1007/s12264-022-00934-6.
[2] Ye H, Robak LA, Yu M, Cykowski M, Shulman JM. Genetics and pathogenesis of Parkinson's syndrome. Annu Rev Pathol 2023;18:95–121. doi: https://doi.org/10.1146/annurev-pathmechdis-031521-034145.
[3] Elkouzi A, Vedam-Mai V, Eisinger RS, Okun MS. Emerging therapies in Parkinson disease -repurposed drugs and new approaches. Nat Rev Neurol 2019;15:204–23. doi: https://doi.org/10.1038/s41582-019-0155-7.
[4] Simon DK, Tanner CM, Brundin P. Parkinson disease epidemiology, pathology, genetics, and pathophysiology. Clin Geriatr Med 2020;36:1–12. doi: https://doi.org/10.1016/j.cger.2019.08.002.
[5] Hung AY, Schwarzschild MA. Approaches to disease modification for Parkinson's disease: clinical trials and lessons learned. Neurotherapeutics 2020;17:1393–405. doi: https://doi.org/10.1007/s13311-020-00964-w.
[6] Piccinin E, Sardanelli AM, Seibel P, Moschetta A, Cocco T, Villani G. PGC-1s in the spotlight with Parkinson's disease. Int J Mol Sci 2021:22. doi: https://doi.org/10.3390/ijms22073487.
[7] Li X, Feng Y, Wang XX, Truong D, Wu YC. The critical role of SIRT1 in Parkinson's disease: mechanism and therapeutic considerations. Aging Dis 2020;11(1608–22). doi: https://doi.org/10.14336/ad.2020.0216.
[8] Chen Y, Jiang Y, Yang Y, Huang X, Sun C. SIRT1 protects dopaminergic neurons in Parkinson's disease models via PGC-1α-mediated mitochondrial biogenesis. Neurotox Res 2021;39:1393–404. doi: https://doi.org/10.1007/s12640-021-00392-4.
[9] Fan F, Li S, Wen Z, Ye Q, Chen X, Ye Q. Regulation of PGC-1α mediated by acetylation and phosphorylation in MPP+ induced cell model of Parkinson's disease. Aging (Albany NY) 2020;12(9461–74). doi: https://doi.org/10.18632/aging.103219.
[10] Sun Z, Ma X, Yang H, Chen S, He S, Sun R, et al. Characterization of Age-dependent behavior deficits in the PGC-1α knockout mouse, in relevance to the Parkinson's disease model. Neuroscience 2020;440:39–47. doi: https://doi.org/10.1016/j.neuroscience.2020.05.015.
[11] Zheng B, Liao Z, Locascio JJ, Lesniak KA, Roderick SS, Watt ML, et al. PGC-1alpha, a potential therapeutic target for early intervention in Parkinson's disease. Sci Transl Med 2010;2:52ra73. doi: https://doi.org/10.1126/scitranslmed.3001059.
[12] Mudo G, Makela J, Di Liberto V, Tselykh TV, Olivieri M, Piepponen P, et al. Transgenic expression and activation of PGC-1alpha protect dopaminergic neurons in the MPTP mouse model of Parkinson's disease. Cell Mol Life Sci 2012;69:1153–65. doi: https://doi.org/10.1007/s00018-011-0850-z.
[13] Ye Q, Huang W, Li D, Si E, Wang J, Wang Y, et al. Overexpression of PGC-1α influences mitochondrial signal transduction of dopaminergic neurons. Mol Neurobiol 2016;53:3756–70. doi: https://doi.org/10.1007/s12035-015-9299-7.
[14] Ciron C, Zheng L, Bobela W, Knott GW, Leone TC, Kelly DP, et al. PGC-1α activity in nigral dopamine neurons determines vulnerability to α-synuclein. Acta Neuropathol Commun 2015;3:16. doi: https://doi.org/10.1186/s40478-015-0200-8.
[15] Das NR, Vaidya B, Khare P, Bishnoi M, Sharma SS. Combination of peroxisome proliferator-activated receptor gamma (PPARγ) agonist and PPAR gamma co-activator 1α (PGC-1α) activator ameliorates cognitive deficits, oxidative stress, and inflammation in rodent model of Parkinson's disease. Curr Neurovasc Res 2021;18:497–507. doi: https://doi.org/10.2174/1567202619666211217140954.
[16] Wang Y, Gao L, Chen J, Li Q, Huo L, Wang Y, et al. Pharmacological Modulation of Nrf2/HO-1 Signaling Pathway as a Therapeutic Target of Parkinson's Disease. Front Pharmacol 2021;12:. doi: https://doi.org/10.3389/fphar.2021.757161757161.
[17] Han K, Jin X, Guo X, Cao G, Tian S, Song Y, et al. Nrf2 knockout altered brain iron deposition and mitigated age-related motor dysfunction in aging mice. Free Radic Biol Med 2021;162:592–602. doi: https://doi.org/10.1016/j.freeradbiomed.2020.11.019.
[18] Zhong Y, Cai X, Ding L, Liao J, Liu X, Huang Y, et al. Nrf2 inhibits the progression of Parkinson's disease by upregulating AABR07032261.5 to repress pyroptosis. J Inflamm Res 2022;15:669–85. doi: https://doi.org/10.2147/jir.S345895.
[19] Pajares M, Cuadrado A, Rojo AI. Modulation of proteostasis by transcription factor NRF2 and impact in neurodegenerative diseases. Redox Biol 2017;11:543–53. doi: https://doi.org/10.1016/j.redox.2017.01.006.
[20] Tonelli C, Chio IIC, Tuveson DA. Transcriptional regulation by Nrf2. Antioxid Redox Signal 2018;29:1727–45. doi: https://doi.org/10.1089/ars.2017.7342.
[21] Niu Y, Zhang J, Dong M. Nrf2 as a potential target for Parkinson's disease therapy. J Mol Med (Berl) 2021;99:917–31. doi: https://doi.org/10.1007/s00109-021-02071-5.
[22] Angelopoulou E, Pyrgelis ES, Piperi C. Neuroprotective potential of chrysin in Parkinson's disease: molecular mechanisms and clinical implications. Neurochem Int 2020;132:. doi: https://doi.org/10.1016/j.neuint.2019.104612104612.
[23] Chen H, Cao J, Zha L, Wang P, Liu Z, Guo B, et al. Neuroprotective and neurogenic effects of novel tetramethylpyrazine derivative T-006 in Parkinson's disease models through activating the MEF2-PGC1α and BDNF/CREB pathways. Aging (Albany NY) 2020;12(14897–917). doi: https://doi.org/10.18632/aging.103551.
[24] Cao J, Guo B, Li S, Zhang X, Zhang X, Zhang G, et al. Neuroprotection against 1-Methyl-4-phenylpyridinium-induced cytotoxicity by naturally occurring polydatin through activation of transcription factor MEF2D. Neuroreport 2021;32:1065–72. doi: https://doi.org/10.1097/wnr.0000000000001696.
[25] Guo B, Hu S, Zheng C, Wang H, Luo F, Li H, et al. Substantial protection against MPTP-associated Parkinson's neurotoxicity in vitro and in vivo by anti-cancer agent SU4312 via activation of MEF2D and inhibition of MAO-B. Neuropharmacology 2017;126:12–24. doi: https://doi.org/10.1016/j.neuropharm.2017.08.014.

[26] McMeekin LJ, Fox SN, Boas SM, Cowell RM. Dysregulation of PGC-1α-dependent transcriptional programs in neurological and developmental disorders: therapeutic challenges and opportunities. Cells 2021:10. doi: https://doi.org/10.3390/cells10020352.
[27] Ryan SD, Dolatabadi N, Chan SF, Zhang X, Akhtar MW, Parker J, et al. Isogenic human iPSC Parkinson's model shows nitrosative stress-induced dysfunction in MEF2-PGC1α transcription. Cell 2013;155:1351–64. doi: https://doi.org/10.1016/j.cell.2013.11.009.
[28] Huang L, Zhong X, Qin S, Deng M. Protocatechuic acid attenuates β-secretase activity and okadaic acid-induced autophagy via the Akt/GSK-3β/MEF2D pathway in PC12 cells. Mol Med Rep 2020;21:1328–35. doi: https://doi.org/10.3892/mmr.2019.10905.
[29] Wang X, She H, Mao Z. Phosphorylation of neuronal survival factor MEF2D by glycogen synthase kinase 3beta in neuronal apoptosis. J Biol Chem 2009;284:32619–26. doi: https://doi.org/10.1074/jbc.M109.067785.
[30] Gong X, Tang X, Wiedmann M, Wang X, Peng J, Zheng D, et al. Cdk5-mediated inhibition of the protective effects of transcription factor MEF2 in neurotoxicity-induced apoptosis. Neuron 2003;38:33–46. doi: https://doi.org/10.1016/s0896-6273(03)00191-0.
[31] Sun Y, Jiang J, Zhang Z, Yu P, Wang L, Xu C, et al. Antioxidative and thrombolytic TMP nitrone for treatment of ischemic stroke. Bioorg Med Chem 2008;16:8868–74. doi: https://doi.org/10.1016/j.bmc.2008.08.075.
[32] Lees KR, Zivin JA, Ashwood T, Davalos A, Davis SM, Diener HC, et al. NXY-059 for acute ischemic stroke. N Engl J Med 2006;354:588–600. doi: https://doi.org/10.1056/NEJMoa052980.
[33] Bi WF, Yang HY, Liu JC, Cheng TH, Chen CH, Shih CM, et al. Inhibition of cyclic strain-induced endothelin-1 secretion by tetramethylpyrazine. Clin Exp Pharmacol Physiol 2005;32:536–40. doi: https://doi.org/10.1111/j.1440-1681.2005.04227.x.
[34] Lu C, Zhang J, Shi X, Miao S, Bi L, Zhang S, et al. Neuroprotective effects of tetramethylpyrazine against dopaminergic neuron injury in a rat model of Parkinson's disease induced by MPTP. Int J Biol Sci 2014;10:350–7. doi: https://doi.org/10.7150/ijbs.8366.
[35] Xu D, Duan H, Zhang Z, Cui W, Wang L, Sun Y, et al. The novel tetramethylpyrazine bis-nitrone (TN-2) protects against MPTP/MPP+-induced neurotoxicity via inhibition of mitochondrial-dependent apoptosis. J Neuroimmune Pharmacol 2014;9:245–58. doi: https://doi.org/10.1007/s11481-013-9514-0.
[36] Xu DP, Zhang K, Zhang ZJ, Sun YW, Guo BJ, Wang YQ, et al. A novel tetramethylpyrazine bis-nitrone (TN-2) protects against 6-hydroxyldopamine-induced neurotoxicity via modulation of the NF-kappaB and the PKCalpha/PI3-K/Akt pathways. Neurochem Int 2014;78:76–85. doi: https://doi.org/10.1016/j.neuint.2014.09.001.
[37] Zhao H, Xu ML, Zhang Q, Guo ZH, Peng Y, Qu ZY, et al. Tetramethylpyrazine alleviated cytokine synthesis and dopamine deficit and improved motor dysfunction in the mice model of Parkinson's disease. Neurol Sci 2014;35:1963–7. doi: https://doi.org/10.1007/s10072-014-1871-9.
[38] Maples KR, Green AR, Floyd RA. Nitrone-related therapeutics: potential of NXY-059 for the treatment of acute ischaemic stroke. CNS Drugs 2004;18:1071–84. doi: https://doi.org/10.2165/00023210-200418150-00003.
[39] Zivin JA. Clinical trials of neuroprotective therapies. Stroke 2007;38:791–3. doi: https://doi.org/10.1161/01.STR.0000252090.44428.82.
[40] Zhang Z, Zhang G, Sun Y, Szeto SS, Law HC, Quan Q, et al. Tetramethylpyrazine nitrone, a multifunctional neuroprotective agent for ischemic stroke therapy. Sci Rep 2016;6:37148. doi: https://doi.org/10.1038/srep37148.
[41] Zhang G, Zhang T, Wu L, Zhou X, Gu J, Li C, et al. Neuroprotective effect and mechanism of action of tetramethylpyrazine nitrone for ischemic stroke therapy. Neuromolecular Med 2018;20:97–111. doi: https://doi.org/10.1007/s12017-018-8478-x.
[42] Zhang T, Gu J, Wu L, Li N, Sun Y, Yu P, et al. Neuroprotective and axonal outgrowth-promoting effects of tetramethylpyrazine nitrone in chronic cerebral hypoperfusion rats and primary hippocampal neurons exposed to hypoxia. Neuropharmacology 2017;118:137–47. doi: https://doi.org/10.1016/j.neuropharm.2017.03.022.
[43] Zhang G, Zhang T, Li N, Wu L, Gu J, Li C, et al. Tetramethylpyrazine nitrone activates the BDNF/Akt/CREB pathway to promote post-ischaemic neuroregeneration and recovery of neurological functions in rats. Br J Pharmacol 2018;175:517–31. doi: https://doi.org/10.1111/bph.14102.
[44] Luo X, Yu Y, Xiang Z, Wu H, Ramakrishna S, Wang Y, et al. Tetramethylpyrazine nitrone protects retinal ganglion cells against N-methyl-d-aspartate-induced excitotoxicity. J Neurochem 2017;141:373–86. doi: https://doi.org/10.1111/jnc.13970.
[45] Zhang G, Zhang F, Zhang T, Gu J, Li C, Sun Y, et al. Tetramethylpyrazine nitrone improves neurobehavioral functions and confers neuroprotection on rats with traumatic brain injury. Neurochem Res 2016;41:2948–57. doi: https://doi.org/10.1007/s11064-016-2013-y.
[46] Zhou X, Zhu L, Wang L, Guo B, Zhang G, Sun Y, et al. Protective effect of edaravone in primary cerebellar granule neurons against iodoacetic acid-induced cell injury. Oxid Med Cell Longev 2015;2015:. doi: https://doi.org/10.1155/2015/606981606981.
[47] Frank LE, Caldera-Siu AD, Pothos EN. Primary dissociated midbrain dopamine cell cultures from rodent neonates. J Visual Exp: JoVE 2008. doi: https://doi.org/10.3791/820.
[48] Zhang J, Nuebel E, Wisidagama DR, Setoguchi K, Hong JS, Van Horn CM, et al. Measuring energy metabolism in cultured cells, including human pluripotent stem cells and differentiated cells. Nat Protoc 2012;7:1068–85. doi: https://doi.org/10.1038/nprot.2012.048.
[49] Cheng A, Wan R, Yang JL, Kamimura N, Son TG, Ouyang X, et al. Involvement of PGC-1α in the formation and maintenance of neuronal dendritic spines. 2012;3:1250. 10.1038/ncomms2238.
[50] Guo B, Xu D, Duan H, Du J, Zhang Z, Lee SM, et al. Therapeutic effects of multifunctional tetramethylpyrazine nitrone on models of Parkinson's disease in vitro and in vivo. Biol Pharm Bull 2014;37:274–85. doi: https://doi.org/10.1248/bpb.b13-00743.
[51] Ghosh A, Kanthasamy A, Joseph J, Anantharam V, Srivastava P, Dranka BP, et al. Anti-inflammatory and neuroprotective effects of an orally active apocynin derivative in pre-clinical models of Parkinson's disease. J Neuroinflammation 2012;9:241. doi: https://doi.org/10.1186/1742-2094-9-241.
[52] Finkelstein DI, Stanic D, Parish CL, Drago J, Horne MK. Quantified assessment of terminal density and innervation. Curr Protoc Neurosci 2004;Chapter 1:Unit 1 13. 10.1002/0471142301.ns0113s27.
[53] Sun YW, Liao KY, Li S, Zhang ZJ, Yu P, Wang YQ. Pharmacokinetic analysis of tetramethylpyrazine Bis-nitrone TN-2 in rats and its protein binding in vitro. Lett Drug Des Discov 2014;11:770–7. doi: https://doi.org/10.2174/15701808116661401212346608.